Chinese Chemical Letters 32 (2021) 2715–2728

Contents lists available at ScienceDirect

Chinese Chemical Letters

journal homepage: www.elsevier.com/locate/cclet

Review

Nanozymes for regulation of reactive oxygen species and disease therapy

Yujie Dai[a,b], Yiming Ding[a,c], Linlin Li[a,b,c,*]

[a] Beijing Institute of Nanoenergy and Nanosystems, Chinese Academy of Sciences, Beijing 101400, China
[b] School of Nanoscience and Technology, University of Chinese Academy of Sciences, Beijing 100049, China
[c] Center on Nanoenergy Research, School of Chemistry and Chemical Engineering, School of Physical Science and Technology, Guangxi University, Nanning 530004, China

ARTICLE INFO

Article history:
Received 10 January 2021
Received in revised form 12 March 2021
Accepted 15 March 2021
Available online 16 March 2021

Keywords:
Nanozyme
Reactive oxygen species (ROS)
Cancer therapy
Peroxidase
Oxidases
Photodynamic therapy

ABSTRACT

With high catalytic activity and stability, nanozymes have huge advantage in generating or eliminating the reactive oxygen species (ROS) due to their intrinsic enzyme-mimicking abilities, therefore attracting wide attention in ROS-related disease therapy. To better design nanozyme-based platforms for ROS-related biological application, we firstly illustrate the catalytic mechanism of different activities, and then introduce different strategies for using nanozymes to augment or reduce ROS level for the applications in cancer therapy, pathogen infection, neurodegeneration, *etc*. Finally, the challenges and future opportunities are proposed for the development and application of nanozymes.

1. Introduction

Natural enzymes participate in the processes of life activities *via* biocatalysis, such as tissue repair [1], cell metabolism [2], anti-inflammation [3] and detoxification [4,5]. Essentially, most natural enzymes are made of proteins or RNA [6]. For realizing engineered applications, the natural enzymes are complicated to purification, costly to use, hard to store, unable to modify and sensitive to the environmental conditions (*e.g.*, pH and temperature), which leads to the restriction in applications. Very recently, nanomaterials with biocatalytic performances have been discovered and explosively developed as possible substitutes for natural enzymes for a train of bioapplications [7]. The term "nanozymes" was firstly proposed by Scrimin and coworkers in 2004 [8]. Nanozymes refer to those artificial nanomaterials that can mimic the activity of natural enzymes. Specifically, in 2007, Yan's group had done pioneered work of discovering the intrinsic peroxidase-like activity of Fe_3O_4 nanoparticles [9]. Since then, considerable achievements have been made in this area with the rapid advances of nanotechnology and nanomaterials. Compared with those natural enzymes, nanozymes have their irreplaceable advantages such as high stability, low cost, tunable catalytic activity, and convenient modification. These superiorities endow nanozymes with enormous application potentials in biosensors [10], pollutant removal [11], anti-bacteria [12], antioxidant [13], cancer therapy [14] and tissue regeneration [15].

Reactive oxygen species (ROS) are natural byproducts of cellular metabolism. ROS can be divided into two categories: free radicals, including singlet oxygen ($^1O_2$), hydroxyl ($HO^{\bullet}$), superoxide ($O_2^{\bullet-}$), hydroperoxyl ($HO_2^{\bullet}$), and nonradicals, such as hydrogen peroxide (H_2O_2) and hypochlorous acid (HOCl). Most of the intracellularly generated ROS come from mitochondria [16], and the other main sources are endoplasmic reticulum (ER), peroxisomes, microsomes, *etc.* [17]. Under normal physiological conditions, the endogenic ROS level is regulated by a series of antioxidant enzymes, keeping it in a dynamic equilibrium. ROS with a moderate level plays multiple roles in body, especially in cellular signal transduction [18]. However, if the ROS concentration is above a normal concentration, it may interfere the normal cell signaling or cause oxidative stress to damage the cells [17]. In cells, the main targets of ROS are nucleic acids, proteins, lipids and sugars [19]. Researches have proved that the intracellular oxidative stress is related to a number of diseases, such as cancer [20], aging [21,22], inflammation [23], diabetes [24,25] and neurodegeneration [26]. Thus, how to control the balance of ROS level in cells and tissues is an urgent challenge to maintain the redox homeostasis. On the other hand, due to their highly toxic nature [27], ROS can be

* Corresponding author at: Beijing Institute of Nanoenergy and Nanosystems, Chinese Academy of Sciences, Beijing 101400, China.
E-mail address: lilinlin@binn.cas.cn (L. Li).

https://doi.org/10.1016/j.cclet.2021.03.036
1001-8417/

applied to kill pathogens or cancer cells, in which an increase in ROS concentration over the threshold could directly kill the detrimental cells. For recent years, with the development of nanotechnology and advances in ROS-relevant nanomaterials, many ROS-mediated therapeutic modalities have emerged to treat the infectious diseases and cancers, such as photodynamic therapy (PDT) [28], sonodynamic therapy (SDT) [29], chemodynamic therapy (CDT) [30], and radiotherapy (RT) [31]. Therefore, augment or reduction of ROS with nanotechnology and nanomaterials is emerging strategy to treat different diseases.

Nanozymes, with the intrinsic properties to mimic natural enzymes, have great promise for modulating the intracellular ROS level. On the one hand, some nanozymes with the activities of catalase (CAT) [32], superoxide dismutase (SOD) [33] and glutathione peroxidase (GPx) [34] can efficiently act as antioxidants to scavenge the excessive amount of ROS. On the other hand, nanozymes with oxidase (OXD) [35] and peroxidase (POD) [36] activities can catalyze the generation of ROS as products or intermediate products to elevate ROS level for disease treatment. Recently, several reviews have comprehensively illustrated the construction and application of nanozyme based systems [37,38]. However, few review papers have been devoted to discussing the strategies of establishment of nanozyme-based nanoplatforms toward the regulation of ROS for disease therapy. To highlight the significance of nanozymes in modulating ROS level for therapeutic purpose, this review aims to elaborate how to design nanozymes for increasing or decreasing ROS at a desired location. First, the type and mechanism of frequently used nanozymes is discussed in detail. Then, the strategies for upregulation and downregulation of ROS with engineered nanomaterials are introduced, including the nanozymes along strategies and synergetic nanozyme strategies. This review also summarizes current challenges and proposes future perspectives for the development of nanozymes for disease therapy. We believe it would provide some inspiration for future design and application of nanozymes.

2. Catalytic mechanism of nanozymes

Although the exploitations and applications of nanozymes have been widely explored for recent years, their kinetics and mechanisms still remain unclear. The understanding of mechanisms from an atomic or molecular level is critical to catch on the essence of catalytic processes, as well as the screening, designing, optimization and application of the nanozymes. To better disclose the nature of nanozymes, increasing researches have been done to discuss the detailed mechanisms [39–41]. As the catalysis often has complicated chemical environment and the reaction intermediates are difficult to capture and analyze, it is difficult to figure out the exact processes and mechanisms. Therefore, most of the theoretical researches are based on first-principal method [42,43], which does not require empirical parameters but calculate the molecular energy according to the interaction principle between nuclei and electrons [44]. Density functional theory (DFT) calculation is one of the most popular methods to conduct theoretical research of nanozymes [44]. This part summarizes the mechanisms of typical nanozymes in terms of different types of nanozymes.

2.1. Peroxidase (POD)

POD-mimicking nanozymes are a group of artificial enzymes that can catalyze the oxidation of substrate in the presence of peroxide. 3,3′,5,5′-Tetramethylbenzidine (TMB) and hydrogen peroxide (H_2O_2) are the popular combination that used as substrates to detect the peroxidase activity. In general, one H_2O_2 absorbed on the surface of a nanozyme could generate two hydroxyl (−OH) species. Then the hydrogen donor TMB provides a hydrogen atom from its amino group to react with the hydroxyl species [39], during which the colorless TMB is oxidized into blue oxidized TMB (oxTMB). This process is illustrated in Fig. 1a. Other researches also point out that the −OH species could be converted into O species to form a peroxidase-O-TMB coordination complex [45]. After donating electrons to the O species, TMB is oxidized, whereas peroxidase-O-TMB is reduced to peroxidase−OH-TMB [46]. Next, the oxTMB desorbs from the peroxidase−OH and another TMB reacts with −OH to recover the nanozyme surface. In this process, free radicals, primarily $HO^{\bullet}$ and also along with $HO_2^{\bullet}$ [47], are produced to endow the highly oxidizing ability of the biomimic peroxidase.

Some other reduced substrates could also be applied to implement a chromogenic reaction, such as: di-azo-aminobenzene

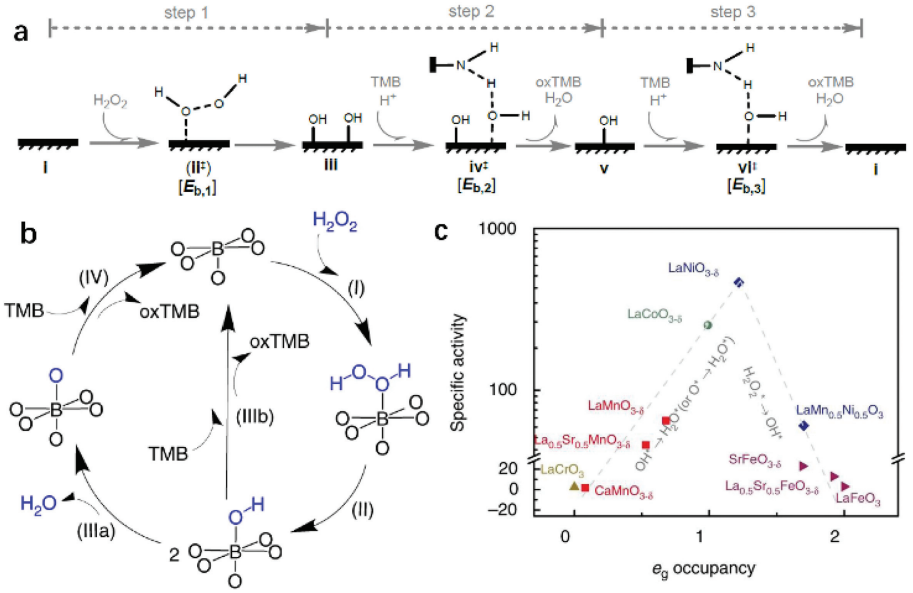

Fig. 1. (a) The proposed mechanism of POD-mimetic catalysis of iron-oxide slabs. Reprinted with permission [39]. Copyright 2020, American Chemical Society. (b) Proposed sub-processes responsible for the oxidation of TMB to oxTMB with the (001) facet of ABO_3 as a peroxidase mimics. (c) Specific peroxidase-like activities of perovskite TMOs plotted as a function of e_g occupancy. Reprinted with permission [45]. Copyright 2019, Nature Publishing Group.

(DAB), *o*-phenylenediamine (OPD) and 2,2′-azino-bis-(3-ethylbenzthiazoline-6-sulfonic acid) (ABTS) [48]. To overcome the poor substrate selectivity and specificity, Liu's group employed molecularly imprinted polymers to create substrate binding pockets on the surface of Fe_3O_4 nanozymes [49]. With the decoration of imprinted charges-enhanced monomers as specific binding pockets to recognize the substrates, the selectivity of Fe_3O_4 NPs was increased for 100 folds than reported before.

For recent years, a large variety of nanomaterials have been reported to have the catalytic ability of natural enzymes. However, most nanozymes were selected through a trial-and-error strategy. There was no exact indicators or parameters to search for nanomaterials with the specific enzyme-like property. In 2019, Wei's group initially identified that the e_g occupancy (*i.e.*, the D-electron population of the e_g (σ^*) anti-bonding orbitals associated with the transition metal sites) could serve as a descriptor for selecting the transition metal oxides (TMO)-based peroxidase mimics (Fig. 1b) [45]. According to the DFT calculations, they concluded that the perovskite TMOs with an e_g occupancy of 1.2 exhibited the highest peroxidase activity, while those with 0 or 2 had a negligible activity (Fig. 1c). Recently, Gao's group also used DFT calculation to indicate the peroxidase activity of nanoparticles [39]. Their calculation showed that both $E_{r,1}$ (the reaction energy of step 1 in Fig. 1a) and $E_{ads,OH}$ (the surface adsorption energy of hydroxyl radical) could act as the descriptors. The nanomaterials would have a POD-like activity when their $E_{r,1}$ is in the energy range from −3.6 eV to −0.3 eV or the $E_{ads,OH}$ is from −3.5 eV to −1.6 eV, and their maximum catalytic activity could be achieved when $E_{r,1}$ = −2.1 eV or $E_{ads,OH}$ = −2.6 eV, respectively.

2.2. Oxidases

Natural oxidases can catalyze the redox reaction between dissolved oxygen and a substrate to produce H_2O or hydrogen peroxide. The family of oxidases has many members, such as glucose oxidase (GOx), sulfite oxidase (SuOx), lactate oxidase (LOx), uric acid oxidase (UOx), amino acid oxidase (AAO), *etc*. Different kinds of oxidases target different substrates. For example, GOx catalyzes *β*-D-glucose into gluconic acid and H_2O_2 [50], and SuOx converts toxic sulfite into bio-safe sulfate [51]. The produced H_2O_2 is a member of ROS family and plays an important role in cell metabolism and signal transduction. It is much more stable than some free radicals and can easily pass cell membrane to react with free ferrous ions in the cells *via* Fenton reaction for generating more active radicals to kill the cells [52,53].

In 2004, Rossi *et al.* unveiled the intrinsic oxidase activity of naked gold nanoparticles [54]. Whereafter, they proposed the mechanism of glucose oxidation with the Au NPs (Fig. 2a) [55]. In detail, hydrated glucose anion reacted with the surface atoms on gold NPs to form electron-rich gold species. These gold species formed a bridge intermediate Au^{+}-O_2^{-} or Au^{2+}-O_2^{2-}, and two electrons were transferred from glucose to oxygen to generate gluconic acid and H_2O_2. Another research based on the oxidase mechanism of noble metal NPs extracted the reactions as the following Eqs. 1 and 2 [56]: Namely, metal NPs decomposed O_2 into two O* adatoms, which had a strong ability to abstract hydrogen atoms from the substrate (S) to yield H_2O_2 and oxidize the substrate.

$$O_2 = 2O^* \quad (1)$$

$$O^* + S \rightarrow H_2O^* + S_{OX} \quad (2)$$

2.3. Catalase (CAT)

Catalase-mimick nanozymes can directly decompose H_2O_2 into H_2O and O_2 (Eq. 3). Both peroxidase and catalase take H_2O_2 as a substrate. However, catalase decomposes H_2O_2 without producing toxic ROS, which means it could effectively serve as an antioxidant. Up to now, many metal and metal oxide nanomaterials have been found to possess catalase activity, such as Ir [57], Pt [58], CeO_2 [59],

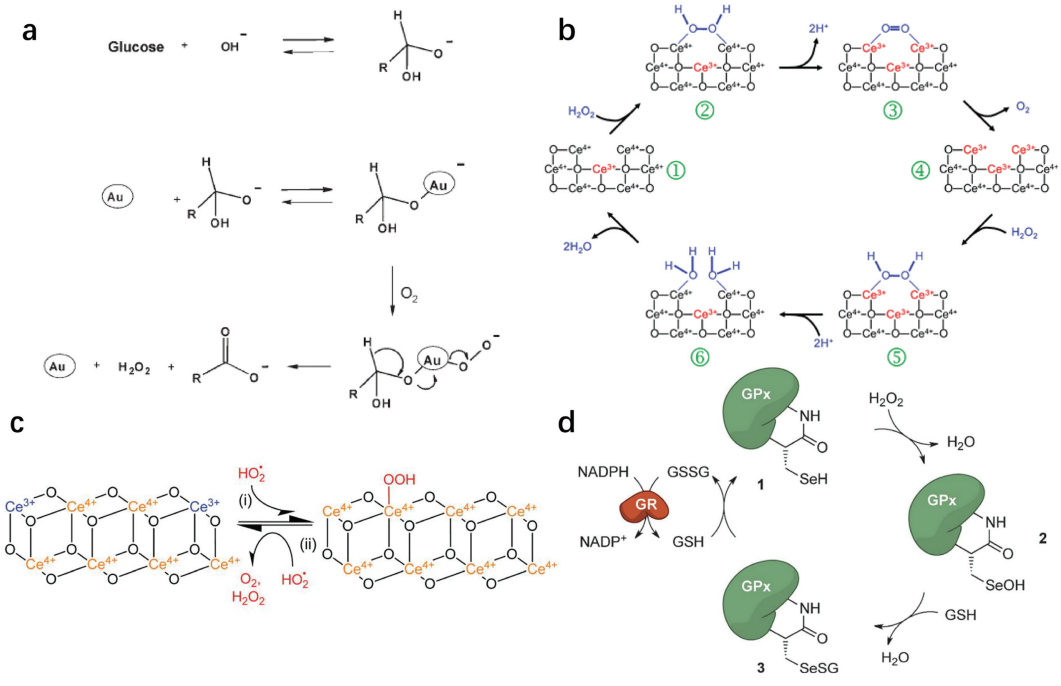

Fig. 2. (a) The oxidase catalytic mechanism of Au NPs. Reprinted with permission [55]. Copyright 2006. John Wiley and Sons. (b) A model of the reaction mechanism for the complete dismutation of hydrogen peroxide. Reprinted with permission [64]. Copyright 2011 Royal Society of Chemistry. (c) Catalytic mechanisms for the SOD-mimetic activity of nanoceria. Reprinted with permission [41]. Copyright 2019 Royal Society of Chemistry. (d) Proposed catalytic cycle of glutathione peroxidase (GPx) for the reduction of hydrogen peroxide and regeneration of glutathione (GSH) using glutathione reductase (GR). Reprinted with permission [84]. Copyright 2015, John Wiley and Sons.

Mn_3O_4 [60].

$$2H_2O_2 \rightarrow O_2 + 2H_2O \quad (3)$$

Among various catalase nanozymes, nanoceria is widely explored due to its high biocompatibility and antioxidant property [61]. Pirmohamed's group identified that the catalase-mimetic activity of nanoceria was dependent on the redox-state ratios of Ce [62]. Further researches acclaimed that a low Ce^{3+}/Ce^{4+} ratio subserved nanoceria's CAT activity whereas a high Ce^{3+}/Ce^{4+} ratio subserved SOD activity [63]. Ghibelli *et al*. illustrated the detailed mechanism of catalase-like nanoceria (Fig. 2b). That is, H_2O_2 first binds to the oxygen vacancy sites on the Ce^{4+} surface that then reduces the vacancy to release O_2 and form Ce^{3+}. Subsequently, another H_2O_2 attaches to the oxygen vacancy again to oxidize Ce^{3+} and regenerate Ce^{4+} and produce H_2O [64]. With a high concentration of H_2O_2, hydroperoxo/peroxo species may appear due to the chelating between Ce^{3+} and H_2O_2 [65]. However, those peroxide species are chemically stable and would not cause a damage to cells/tissues/bodies like that induced by hydroxyl radicals [66]. This process could be summarized in Eqs. 4–7 [67]:

$$2Ce^{3+} + H_2O_2 + 2H^+ \rightarrow 2H_2O + 2Ce^{4+} \quad (4)$$

$$Ce^{4+} + H_2O_2 \rightarrow Ce^{3+} + H^+ + HOO^{\bullet} \quad (5)$$

$$Ce^{4+} + HOO^{\bullet} \rightarrow Ce^{3+} + O_2 + H^+ \quad (6)$$

$$2Ce^{4+} + H_2O_2 \rightarrow 2Ce^{3+} + O_2 + 2H^+ \quad (7)$$

From DFT calculation and micro-kinetic modeling, Guo *et al*. proposed three possible CAT catalytic mechanisms of Fe_3O_4 nanoparticles (Table 1) [46]: the base-like dissociative mechanism, the acid-like dissociative mechanism, and the bihydrogen peroxide associative mechanism. Their results showed that the acid-like dissociative mechanism was the energetically favorable pathway.

2.4. Superoxide dismutase (SOD)

Superoxide dismutase catalyzes the disproportionation of superoxide radicals to generate H_2O_2 and O_2. Natural SOD enzymes, mainly taking Fe/Mn/Co/Ni as the active sites [68], exit in different counterparts of cells (*e.g.*, mitochondria, cytosol, and peroxisomes) [69] to maintain the intracellular redox equilibrium [70]. Therefore, many metal ions-included nanozymes are designed to mimic SOD [71,72].

SOD catalyzes substrate through a Ping-Pong mechanism with $O_2^{\bullet -}$ alternately reducing the oxidized metal ions and then oxidizing the reduced metal ions [73]. $O_2^{\bullet -}$ is easy to catch a proton from water to produce a protonated $HO_2^{\bullet}$ (Eq. 8). The $HO_2^{\bullet}$ acts as both a one-electron reductant and an oxidant. So two $HO_2^{\bullet}$ react to generate H_2O_2 and O_2 (Eq. 9). The SOD catalytic process of nanoceria could be divided into two steps (Fig. 2c) [41]. (1) The first $HO_2^{\bullet}$ absorbs on the nanoceria surface. (2) After electrons transferring from Ce^{3+}, the second $HO_2^{\bullet}$ reacts to produce H_2O_2 and O_2. Self and coworkers proved that a decrease in the Ce^{3+}/Ce^{4+} ratio directly resulted in the loss of SOD activity [74].

$$O_2^{\bullet -} + H_2O \rightleftharpoons HO_2^{\bullet} + OH^- \quad (8)$$

$$HO_2^{\bullet} + HO_2^{\bullet} \rightarrow H_2O_2 + O_2 \quad (9)$$

To illustrate the role of SOD nanozymes, Gao *et al*. revealed that the adsorption and rearrangement of protonated $HO_2^{\bullet}$ on the surface of metal-based SOD nanozymes was critical to the catalysis [56]. Once two $HO_2^{\bullet}$ groups rearranged on the surface, the activation energy barriers became very low, which facilitated the conversion of $HO_2^{\bullet}$ into O_2 and H_2O_2.

2.5. Glutathione peroxidase (GPx)

GSH is an abundant endogenous thiol and serves as a reductant in cells [75,76]. Natural GPx is known to manipulate the redox homeostasis by reducing excessive H_2O_2 or organic hydroperoxide to H_2O [77,78]. GPx includes 8 types (GPx 1–8) and distributes in different cellular compartments, for example, GPx1 in cytosol and mitochondria, GPx2 in intestinal epithelium, and GPx3 in cytoplasm [79]. Recent researches show that GPx4 is an important participant in ferroptosis, because it can inhibit lipid peroxidation to protect cell membrane [80,81].

The active center of natural GPx is selenocysteine [82]. Thus, Se-based nanozymes are excellent candidates for anti-oxidants [34,83]. The specific mechanism of natural selenium GPx has three steps (Fig. 2d) [84]: (1) H_2O_2 reacts with the selenol moiety (Enz-SeH) to form a selenenic acid (Enz-SeOH); (2) This selenenic acid then reacts with GSH to form a selenenyl sulfide (E-Se-SG); (3) At last, a second GSH cleavages the selenium–sulfur bond and recovers the selenol moiety. In the third step, the NADPH-dependent glutathione reductase (GR) is needed to maintain the GSH level by reducing glutathione disulfide (GSSG) back to GSH.

The catalysis of GPx nanozymes can be divided into two steps: an oxidative half-reaction and a reductive half-reaction. Qu *et al*. illustrated the mechanism of graphene oxide-based selenium (GO-Se) nanozyme [85]: First, nanoselenium reacted with H_2O_2 to obtain a selenium oxide intermediate. Then, this intermediate returned to its original state by oxidizing GSH to GSSG. Except for selenium, Mn_3O_4 [86] and vanadia can also mimic GPx. Mugesh and co-workers analyzed the mechanistic details about the interaction of GSH on a V surface [87]. They also found that the size, morphology, and surface-exposed crystal facets of nanomaterials can influence the GPx activity of V_2O_5 [88]. Besides, the activity of GPx was closely related to the valence ratio. That is, Mn_3O_4 with a higher Mn^{3+}/Mn^{2+} ratio exhibited a higher GPx activity [86].

Table 1
CAT catalytic mechanisms of Fe_3O_4 nanoparticles.

Base-like dissociative mechanism	Acid-like dissociative mechanism	Associative mechanism
H_2O_2 (g) + * → H_2O_2*	H_2O_2 (g) +* → OOH* + H*	$2H_2O_2$ (g) + 2* → OH* + HOO* + H_2O (g)
H_2O_2 (g) + * → OH* + HO*	OOH* + H* + * →O* + H_2O (g)	HOO* + * → H* + OO* (g)
2OH* + * → H_2O (g) + O*	H_2O_2 (g) + O* →OH_2O_2*	OO* → O_2 (g) + *
H_2O_2 (g) + O* + * → OOH* + HO*	OH_2O_2* + * →OHOO* + H*	OH* + H* → H_2O (g)
OOH* + HO* + * → O_2 (g) + H_2O (g)	OHOO* + * →OH* + OO*	
	OO* → O_2 (g) + *	
	H* + OH* → H_2O (g)	

Reprinted with permission [46]. Copyright 2019, American Chemical Society.
*Refers to an adsorption site.

3. Nanozymes upregulating ROS for disease therapy

Due to the strong oxidizing property, the augment of ROS has been broadly employed in removing tumors and eliminating pathogens. Nanozymes are talented candidates in constructing ROS generating nanoplatforms as they are capable of transferring chemical energy into internal energy of ROS [89]. For instance, both the product of oxidase (H_2O_2) and the intermediate of peroxidase ($HO^{\bullet}$) are toxic ROS. Consequently, nanozymes can be directly used to enhance ROS production. However, owing to the limited amount of substrates, it is not easy to achieve the desired effects with mere one kind of enzymatic activity. As a result, many nanoplatforms with multi-enzyme activities have been designed to assist to increase ROS. Besides, nanozymes with synergetic therapeutic effect are also widely applied for ROS generation to amplify therapeutic effects. In this part, we highlight the representative strategies for composing ROS-upregulating nanoplatforms. These strategies are significant to supply sufficient ROS for a therapeutic purpose, especially for cancer and pathogen infectious disease.

3.1. Single-enzyme-like strategy

Due to the chemically active substrates and intermediates, nanozymes have fascinating intrinsic properties to regulate ROS. Oxidase-mimic nanozymes catalyze oxygen to produce H_2O_2. As a redox metabolite, H_2O_2 is recently unveiled to be a central hub in regulating oxidative stress and redox signaling [90,91]. Compared with other reactive species, H_2O_2 is relatively long lived and can freely cross cytomembranes and diffuse in cellular compartments [92]. Thus, it is easy to react with other intracellular enzymes or metallic sub-ions (*e.g.*, Fe^{2+}) to generate more toxic free radicals. As a result, oxidase can efficiently increase the ROS level by producing H_2O_2.

Dong and co-workers fabricated a single-atom nanozyme with carbon nanoframe-confined FeN_5 active centers (FeN_5 SA/CNF) to mimic oxidase [93]. The structure of the active sites was similar to the axial ligand–coordinated heme of natural cytocrome P450. Besides, DFT calculation showed that the FeN_5 SA/CNF had the highest calculated adsorption energy and farther O-O distance of the adsorbed $^*O_2$ due to the electron pushing effect of the axial-coordinated N, which made the FeN_5 SA/CNF had a 70-times higher catalytic rate constant than the commercial Pt/C nanomaterials. The enhanced oxidase activity of the FeN_5 SA/CNF could seriously destroy the cell membrane of *Escherichia coli* (*E. coli*) and *Staphylococcus aureus* (*S. aureus*) *to* promote wound healing of the infected tissues.

Apart from oxidase, peroxidase can also up-regulate ROS by producing $HO^{\bullet}$ as an intermediate. With a +2.8 V oxidation potential, $HO^{\bullet}$ possesses excellent ability to catch electrons and thus serves as a powerful oxidant [94]. Liu and co-workers presented a peroxidase-like single-atom nanozyme (PMCS) by using a ZIF-8-derived Zn-N-C single-atom nanocatalyst (Figs. 3a and b) [95]. They compared PMCS under three different temperatures (600 ℃, 800 ℃, and 1000 ℃) and found that PMCS under 800 ℃ pyrolysis had the highest Zn-N percentage (16.24%) (Fig. 3c) and highest POD activity. Through DFT calculation and extended X-ray absorption fine structure (EXAFS) fitting, they concluded that the maximum and average coordination number of single Zn sites in PMCS was 5 and 4.6, respectively, while only the PMCS with an unsaturated four-coordinated structure was active. It could significantly promote wound healing by inhibiting the growth of *P. aeruginosa* up to 99.87% (Figs. 3d and e).

Besides, Liang's work showed that peroxidase-like Fe_3O_4 nanoparticles could significantly suppress tumor growth by a new type of cell lethality, called nanoptosis [96]. According to the research, nanoptosis had morphological and biochemical difference from other types of programed cell death. Quantitative proteomics and RNA sequencing analysis showed that this process was regulated by ATP-citrate lyase (ACLY)-dependent rat sarcoma viral oncogene (RAS) signaling pathway.

Although oxidase and peroxidase nanozyme can directly generate ROS, the limited endogenous oxygen and H_2O_2 resources result in the restricted catalytic efficiency. As a result, it is not easy for applying this kind of single-enzyme mimic nanozyme to acquire enough amount of ROS for efficient therapy. It usually needs extra addition of H_2O_2 [95] or other auxiliary effect [97].

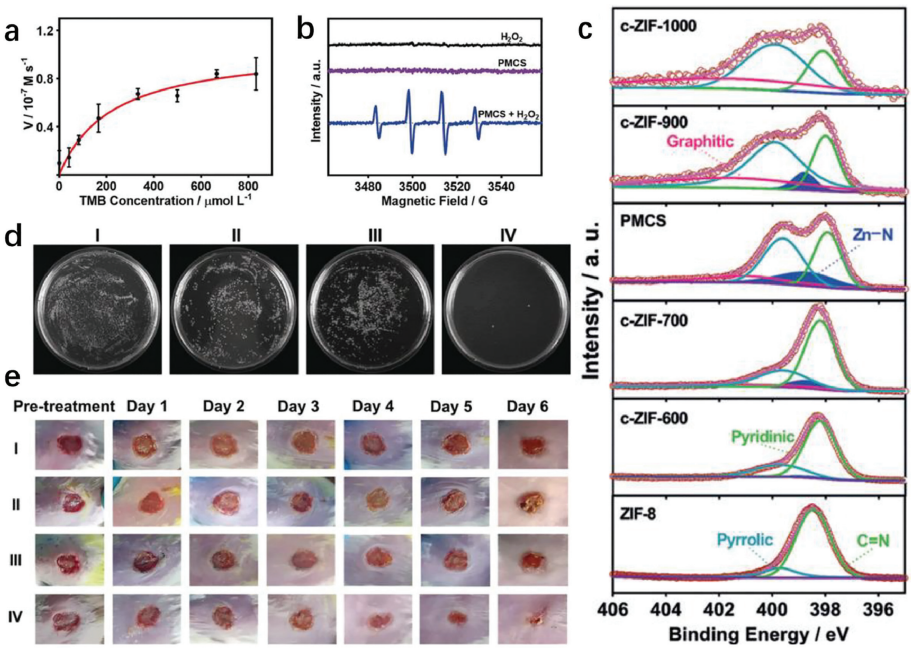

Fig. 3. (a) Model steady-state kinetic assay of the PMCS for TMB. (b) ESR spectra demonstrating $HO^{\bullet}$ generation by H_2O_2. (c) High-resolution N 1s XPS spectra for c-ZIF-1000, c-ZIF-900, the PMCS, c-ZIF-700, c-ZIF-600, and ZIF-8. (d) Photographs of bacterial colonies formed by *P. aeruginosa*. (e) Photographs of the *P. aeruginosa*-infected wound treated after different lengths of time. Reprinted with permission [95]. Copyright 2019, John Wiley and Sons.

3.2. Muti-enzyme-like strategy

To solve this problem, abundant nanomaterials with multi-enzyme-like properties have been explored with two or more enzyme activities, simultaneously. Due to the cascade reaction between different enzyme activities, the product of one reaction could direct act as the substrate of another reaction, so the catalytic process could be prolonged and amplified to generate more ROS. Besides, the synergistic effect between different enzyme activities can also promote the ROS generation. For the past several years, multi-enzyme-like nanozymes are widely investigated for diverse biological applications.

On the one hand, some nanozymes intrinsically have two or more enzyme activities, simultaneously, for example, Au mimicking POD and OXD [98,99], Co/PMCS mimicking GPx, CAT and SOD [100], nitrogen-doped carbon nanozyme mimicking POD, OXD, CAT and SOD [101]. On the other hand, multi-enzyme-like nanomaterials can be achieved by integrating different components with different enzymatic activities into a multifunctional platform. Qu's group firstly constructed a multi-enzyme-like platform (V_2O_5@pDA@MnO_2) to mimic an intracellular antioxidant defense system by using dopamine to assemble V_2O_5 nanowires (mimicking GPx) and MnO_2 nanoparticles (mimicking SOD and CAT) [102] together.

To construct nanozymes with an enhanced ROS generation ability, the most common strategy is to fabricate nanozymes with glucose oxidase and peroxidase activity, as both of them could directly produce ROS. Glucose oxidase can generate H_2O_2, which provides more substrate for peroxidase. In addition, glucose oxidase also catalyzes the generation of gluconic acid. It induces a more acidic environment to improve the activity of peroxidase, as the optimal pH for peroxidase is around 4. For example, Wang's group prepared a Cu_2WS_4 nanocrystals with both oxidase and peroxidase properties, having a high anti-bacterial activity for wound treatment [103]. Moreover, Qu's group also constructed a MOF-based hybrid nanocatalyst by adsorbing natural glucose oxidase on a peroxidase-like two-dimensional (2D) MOF (2D Cu-TCPP(Fe)) nanosheet for *in vivo* wound healing [104].

The combination of oxidase and catalase is also a good strategy to enhance the generation of ROS. Hypoxia is one of the typical characteristics of tumor microenvironment, which greatly limits the therapeutic effects of photodynamic therapy (PDT) and sonodynamic therapy (SDT) that consume O_2. Oxidase depends on oxygen to produce H_2O_2, which also provides substrate for catalase to generate more O_2 back for oxidase. Hence, through the synergetic effects between oxidase and catalase, tumor hypoxia could be vastly relieved to make the therapeutic system be unconstrained by O_2 and H_2O_2. Qu *et al.* developed a biomimetic MnO_2@PtCo nanoflower based on the self-assembly of oxidase-mimicking PtCo with catalase-mimicking MnO_2 [105]. This composite nanozyme could not only relieve hypoxia condition but also induce a ROS-mediated cell apoptosis, which resulted in a remarkable inhibition of tumor growth.

Inspired by natural neutrophil lysosomes, Wang's group integrated SOD and chloroperoxidase (CPO) into a cascade nanogel system (SCNG) for enzyme dynamic therapy (EDT) (Fig. 4a) [106]. CPO is also a peroxidase with the ability to catalyze chloride with H_2O_2 to dominantly produce singlet oxygen. Generally, SOD converted $O_2^{\bullet-}$ to H_2O_2, which provided more substrates for CPO to generate a large amount of $^1O_2$. This nanozyme system built a $^1O_2$-elevating strategy for hypoxic tumor therapy. What is more, they also prepared a metal coordinated polymeric nanogels (MPGs) with SOD and POD activities for ROS-responsive fluorescence imaging [107]. The SOD activity converted the excessive $O_2^{\bullet-}$ in tumors into H_2O_2, which was further applied as fluorescent substrate of POD to realize efficient H_2O_2-responsive fluorescence imaging.

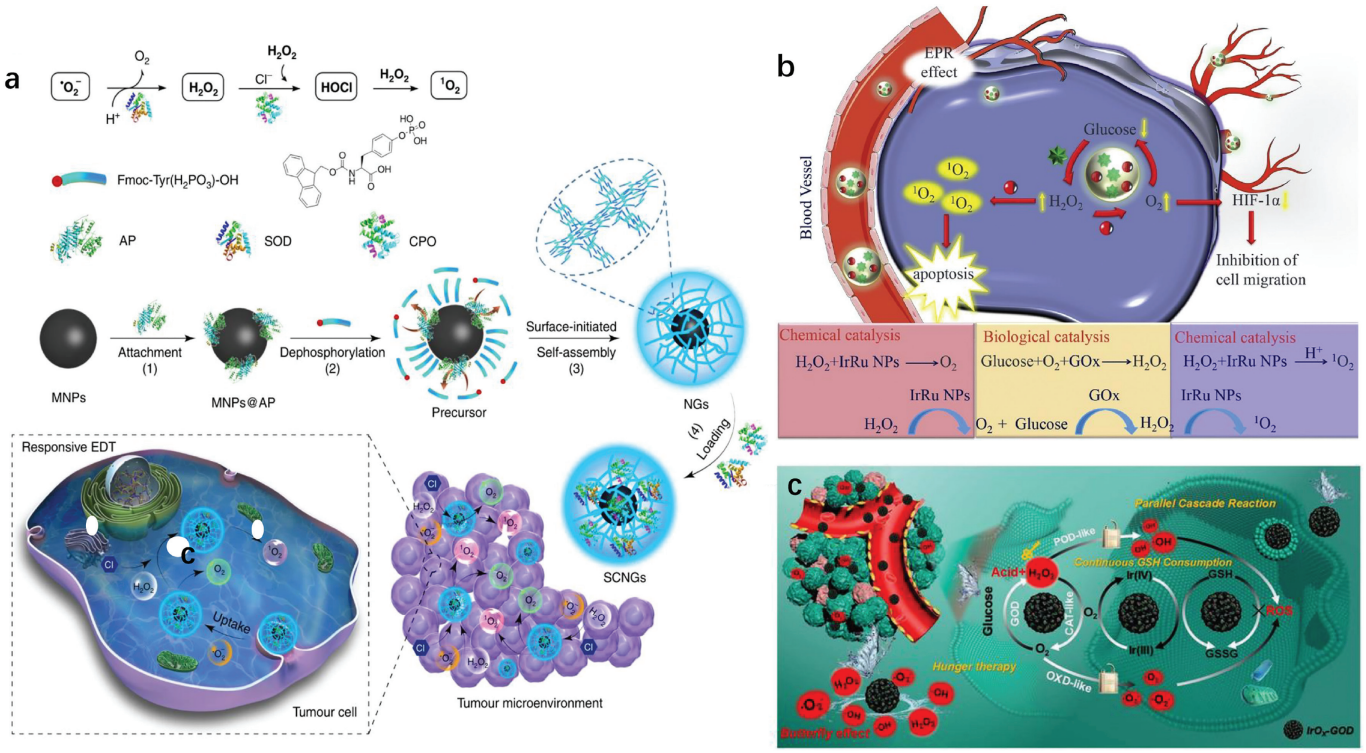

Fig. 4. (a) Scheme of the responsive EDT mechanism and preparation of SCNGs. Reprinted with permission [106]. Copyright 2019, Nature Publishing Group. (b) Schematic illustration of the cycle-like nanosystem IrRu-GOx@PEG NPs including catalyzing glucose depletion, O_2 cycle-like support and starvation therapy for enhanced oxidation therapy in a hypoxic tumor microenvironment. Reprinted with permission [108]. Copyright 2020, Elsevier. (c) Butterfly effect in cancer cells after the introduction of IrOx-GOD NPs into the chaotic tumor system. Reprinted with permission [109]. Copyright 2020, John Wiley and Sons.

Apart from the double-enzyme-mimic nanozymes, nanoplatforms with three kinds of enzyme activities are also widely explored. Liu *et al*. synthesized a multi-enzyme nanoreactor (IrRu-GOx@PEG NPs) by loading GOx on IrRu nanoparticles with the surface modification of polyethylene glycol (PEG) to undergo the GOx, CAT and POD activities (Fig. 4b) [108]. At first, GOx degraded glucose to generate H_2O_2, and then POD and CAT-like IrRu NPs not only converted mildly toxic H_2O_2 into highly toxic ROS, but also catalyzed the formation of O_2 to assist glucose consumption. This nanosystem synergistically combined starvation therapy with oxidation therapy to inhibit breast tumor growth and metastasis.

Nanosystems with 4 kind of enzymes are also reported. Jiang *et al*. loaded GOx on iridium oxide nanoparticles (IrOx) to create a four-enzyme expressed nanozyme (IrOx-GOD) (Fig. 4c): CAT, GOx, OXD, and POD [109]. Firstly, CAT-like activity decomposed the over-produced H_2O_2 into O_2 and then O_2 reacted with glucose to produce glucose acidic and H_2O_2 again, which ensured the continuous supply of O_2 and H_2O_2 and provided an acidic environment to unlock the OXD and POD activities. Next, OXD and POD activities accumulated abundant $HO^{\bullet}$ and $O_2^{\bullet-}$ to cause serious oxidative stress. More importantly, by the self-cyclic valence alternation of Ir^{IV} and Ir^{III}, IrOx could also consume GSH to prevent the anti-oxidation defense. This designed IrOx-GOD reactor leads to a "butterfly effect" to break the self-adaption of cancer cells and eliminate tumors by continuous ROS oxidative stress and starvation therapy.

3.3. Synergy with other therapeutic modalities

3.3.1. PTT-enhanced synergetic therapy

Due to the diversity and complicity of tumor environment, it is hard to generate enough ROS to eliminate tumors without any external assistance. Under this situation, synergetic therapy has been well developed to achieve an enhanced catalytic and therapeutic effect. Photothermal therapy (PTT) has emerged as an effective and non-invasive strategy by selectively converting an incident light into heat with the assistance of photothermal conversion nanomaterials. Specifically, reports have showed that PTT could produce intracellular ROS through direct interaction between shockwaves and surrounding molecules [110], or indirect cellular stress [111]. The heat stress caused from high temperature could also induce oxidative damage by disturbing the mitochondrial homeostasis [112]. Most importantly, light irradiation could significantly promote the enzyme activity and accelerate the enzyme reaction through the photothermal effect [113]. It can generate cytotoxic $HO^{\bullet}$ and $O_2^{\bullet-}$ through direct electron transfer and photothermal-enhanced Fenton reaction [114,115]. For the above reasons, catalysis with synergetic PTT has great potentials to increase intracellular ROS level. Many nanozymes (*e.g.*, Au [116], Cu [117], and Fe_3O_4 [118] NPs) are outstanding PTT candidates due to their strong optical absorption property and high photothermal conversion efficiency.

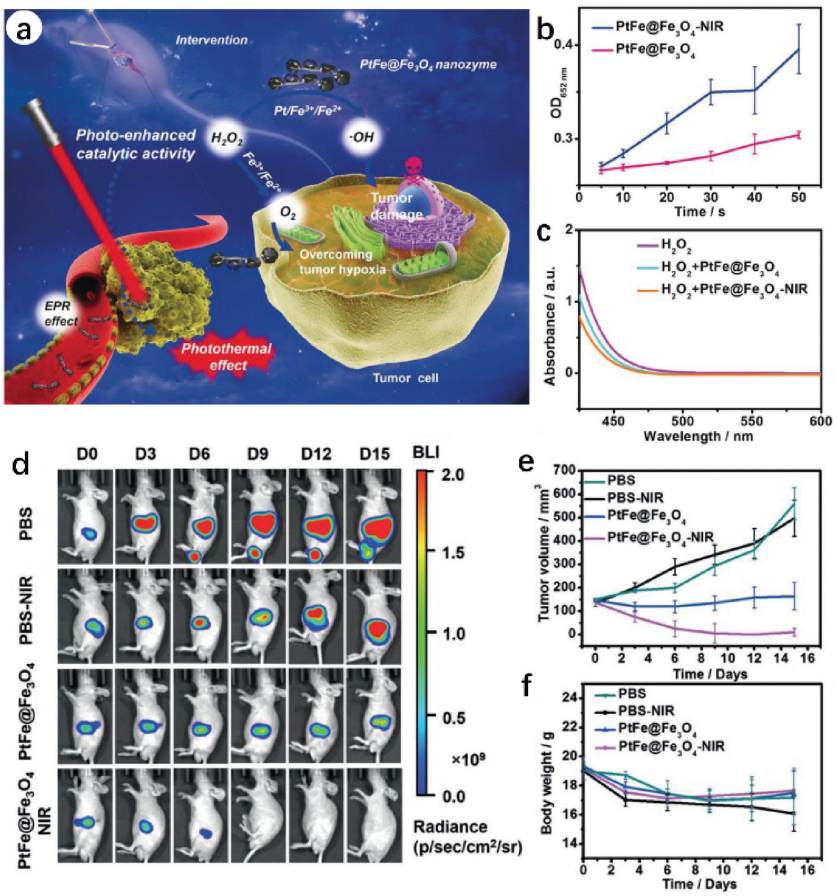

Fig. 5. (a) Schematic of the photo-enhanced tumor catalytic therapy based on the PtFe@Fe_3O_4 nanozyme. (b) Irradiation time-dependent absorbance changes at 652 nm. (c) H_2O_2 consumption in NaAc buffer in the presence of PtFe@Fe_3O_4 NRs and ammonium molybdate. (d) Tumor region at 3 days interval in different groups. (e) Tumor volume of mice in different groups during 15 days of treatments. (f) Body weight of mice in different groups during 15 days of treatments. Reprinted with permission [119]. Copyright 2019, John Wiley and Sons.

Liu and coworkers reported a PtFe@Fe_3O_4 nanorods (NRs) with photo-enhanced peroxidase and catalase activities (Fig. 5a) [119]. They also disclosed the photo-enhanced synergetic catalytic mechanism. As a noble metal, Pt could efficiently convert NIR light into heat because of the surface plasmon resonance (SPR) effect. The SPR effect of PtFe NRs could enhance the electric near-field in the vicinity. Therefore, they hypothesized that the SPR effect of PtFe in PtFe@Fe_3O_4 NRs could inhibit the rapid recombination of photoexcited electron-hole pairs and boost the excitation of electron–hole pairs in Fe_3O_4, thereby helping H_2O_2 accept electrons easily to enhance the catalytic efficiency. The results indicated that both the SPR effect and thermal effect could accelerate the catalytic reaction. The POD and CAT activity of the PtFe@Fe_3O_4 could be significantly improved under the 808 nm NIR laser irradiation (Figs. 5b and c). Owing to the O_2 generation by the CAT activity, this nanozyme could notably overcome tumor hypoxia and reach a tumor inhibition rate of 99.8% towards deep pancreatic cancer (Figs. 5d–f).

Zhang *et al.* also fabricated a transformable hybrid semiconducting polymer nanozyme (HSN) with a 98.9% photothermal conversion efficiency under the NIR II light irradiation [120]. The photothermal transduction could not only trigger cytotoxicity but also potentiate Fenton reaction to increase cellular oxidative stress. Lin's group developed a bacteria-like nanozyme (PEG/Ce-Bi@DMSN) with a satisfactory absorption in the second near-infrared (NIR-II) window [121]. The photothermal conversion efficiency (η) was 36.2% at 1064 nm, which could efficiently convert light into heat to enhance the POD activity, CAT activity, and GSH depletion capability for efficient nanocatalytic cancer therapy.

3.3.2. Photodynamic therapy (PDT)-enhanced synergetic therapy

PDT is one of the most developed ROS-generating treatment method and has been successfully used in clinical applications [28]. After photo irradiation, photosensitizers are activated to react with tissue oxygen, rendering cytotoxic ROS to induce cell death [122,123]. However, tumor hypoxia limits the oxygen resources, which restricts the produce of ROS [124]. Under this situation, to relieve the tumor hypoxia becomes an urgent requirement. Nanozymes with catalase activity can directly decompose H_2O_2 into O_2, which makes it a potential candidate for solving hypoxia. Moreover, some specific nanozymes, such as MOF-based nanozymes, are intrinsic photosensitizers [125] or have strong loading capacity for photosensitizers, which guarantee their photodynamic effect. In addition, nanozymes with multiple enzyme activities could produce ROS. Therefore, the combination of nanozymes with PDT is an optimal choice in cancer therapy.

Zhao and coworkers developed a single-atom nanozyme (OxgenMCC-r SAE) by using catalase-mimicking Ru ions to partially substitute the metal ions in MOFs [126]. The prepared OxgenMC-r SAE had a high chlorin e6 (Ce6) loading capacity due to the intrinsic porous structure of MOFs. The high utilization efficiency of active sites ensured the high H_2O_2 catalytic ability and durability, which allowed it to generate abundant endogenous oxygen for further generating $^1O_2$ and inducing cell apoptosis. This multifunctional nano-catalyst could successfully relieve the hypoxia condition and reduce the tumor volume of 4T1 tumor-bearing mice.

Besides catalase, other kind of enzyme activities also play a vital role as a synergetic way to enhance ROS generation together with PDT. For example, Wu *et al.* used porous porphyrin metal-organic frameworks (PCN) as both a photosensitizer and a substrate to embed catalase-mimicking Pt NPs and glucose oxidase-mimicking Au NPs [14]. Followed by tethering folic acid (FA) on the outer shell, they presented a unique and rationally designed nanoreactor, P@Pt@P-Au-FA (Fig. 6a). The Au NPs could not only deplete glucose to accelerate starving therapy but also provide the substrate H_2O_2 for catalase. Pt NPs were able to catalyze H_2O_2 to generate O_2 for enhancing the O_2-dependent PDT efficiency (Fig. 6b) and potentially accelerate the depletion of intratumoral glucose by the Au NPs (Fig. 6c). Hence, this PCN-supported dual-nanozymes-mimicking nanoreactor showed practically remarkable strengthened antitumor efficiency based on the catalytic cascade reaction (Figs. 6d–f).

3.3.3. Sonodynamic therapy (SDT)-enhanced synergetic therapy

Another noninvasive therapeutic treatment, SDT, employs ultrasound to trigger sonosensitizers for the generation of toxic ROS. Different from phototherapy, SDT has a deeper penetration depth without phototoxicity [29], which makes it a promising therapeutic strategy over PDT [127]. However, the clinical application of SDT is mainly impeded due to the low performance of sonosensitizers [128], tumor hypoxia [129] and high concentration of intracellular GSH [130]. In tumor microenvironment, insufficient oxygenation would directly cause poor production of singlet oxygen. Meanwhile, abundant GSH would consume the as-produced singlet oxygen to protect cells from oxidative damage [130]. Under these circumstances, nanozymes show their special superiority, as catalase could generate oxygen while glutathione peroxidase could reduce GSH [131].

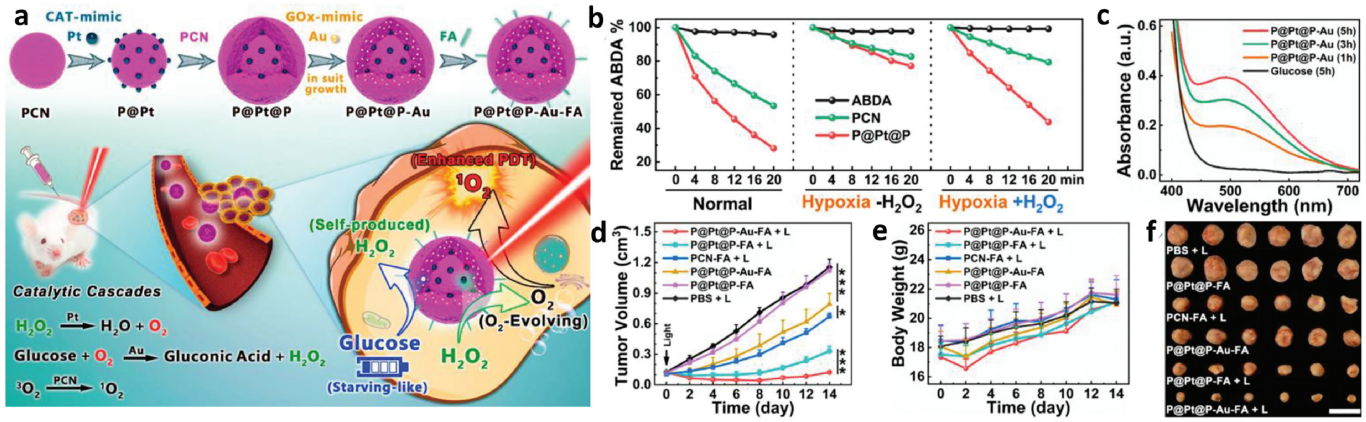

Fig. 6. (a) Schematic illustration of the catalytic cascades-enhanced synergistic cancer therapy driven by dual inorganic nanozymes-engineered porphyrin metal-organic frameworks (PCNs). (b) PDT efficacy of PCN or P@Pt@P under three different conditions upon a 671 nm laser exposure. (c) Glucose oxidase mimicking ability of P@Pt@P-Au determined by UV–vis-NIR spectroscopy. (d) Tumor growth curves, (e) body weight changes and (f) tumor volume picture of the 4T1 tumor-bearing mice. Reprinted with permission [14]. Copyright 2019, American Chemical Society.

Many kinds of nanozymes have been developed to boost the therapeutic effect of SDT. For example, Chen's group constructed an intelligent nanoplatform by using hollow mesoporous organosilica nanoparticles to load sonosensitizers and catalase-like MnOx [132]. The MnOx could decompose H_2O_2 to alleviate tumor hypoxia and oxidize GSH to protect the generated $^1O_2$. Recently, Yang's group firstly reported $PtCu_3$ nanocages as a sonosensitizer with efficient ROS generation property (Figs. 7a and b) [133]. The as-prepared $PtCu_3$ nanocages also acted as both horseradish peroxidase and glutathione peroxidase. On the one hand, its peroxidase activity could catalyze H_2O_2 to produce $HO^{\bullet}$ for CDT (Fig. 7c), increasing the cellular oxidative stress. On the other hand, its GPx activity could deplete GSH (Fig. 7d), further weakening the ROS scavenging capacity of the tumor cells. Moreover, due to the high absorption in the near-infrared region and strong X-ray attenuation ability, $PtCu_3$ nanocages could realize photoacoustic/computed tomography dual-modal imaging during therapy. This multimodal imaging-guided SDT had an excellent performance for curing deep-seated tumors (Figs. 7e–g).

Interestingly, nanozymes could enhance the SDT effect, and meanwhile US could switch on-off the enzyme activity (Fig. 7h). Zheng *et al.* designed a US-switchable nanozyme to augment SDT effect [134]. The nanoplatform (Pd@Pt-T790) was acquired by modifying organic sonosensitizer mesotetra (4-carboxyphenyl) porphine (T790) onto the Pd@Pt nanoplates, which could block their catalase activity. After the US irradiation, the catalase activity was efficiently recovered to generate oxygen for the enhancement of SDT efficiency (Figs. 7i–k). With the assist of photoacoustic imaging and magnetic resonance imaging, the Pd@Pt-T790 SDT nanosystem was successfully applied to eradicate methicillin-resistant *S. aureus* (MRSA)-induced myositis. This controllable "blocking and activating" strategy had particularly important meanings to reduce the potential toxicity and side effects of the nanozymes on normal tissues.

3.3.4. Chemodynamic therapy (CDT)-enhanced synergetic therapy

As mentioned above, both PDT and SDT need exogenous stimuli such as light or ultrasound. In contract, CDT does not require any external intervention. As a local TME-responsive therapeutic modality, CDT is driven by endogenous chemical reaction to promote ROS generation for specific therapeutic outcome [135]. The most common method to achieve CDT is the Fenton reaction between nanomaterials containing Fe^{2+}/Fe^{3+} and overproduced H_2O_2 in tumor [136]. Besides, other transition metals, such as Mn, Cu, Ni, and Co, could also perform a Fenton-like reaction to trigger CDT [137]. Unfortunately, Fenton reaction excessively relies on H_2O_2, but the intratumoral H_2O_2 concentration (around $50-100\times10^{-6}$ mol/L) is too low to generate sufficient ROS [138]. Another question is that the optimal pH for Fe ion mediated Fenton reaction is pH 2–4, while pH in tumor microenvironment is in the range of 6.5–7 [139], which restricts the reaction rates. Moreover, to maintain the homeostasis, the overproduced ROS in the tumor microenvironment often results in the concentration elevation of antioxidant components, such as GSH, to consume H_2O_2. Thus, increase of the local H_2O_2 and the acidity in tumor is one of the pathways to promote Fenton reaction efficiency for increasing CDT therapeutic effect.

In order to promote H_2O_2 generation and inhibit H_2O_2 elimination, Ren's group devised a nanozyme-based H_2O_2 homeostasis disruptor for intensive CDT (Fig. 8a) [140]. The disruptor PZIF67-AT was manufactured by coating the CAT inhibitor 3-amino-1,2,4-triazole (3-AT) and PEG on zeolitic imidazole

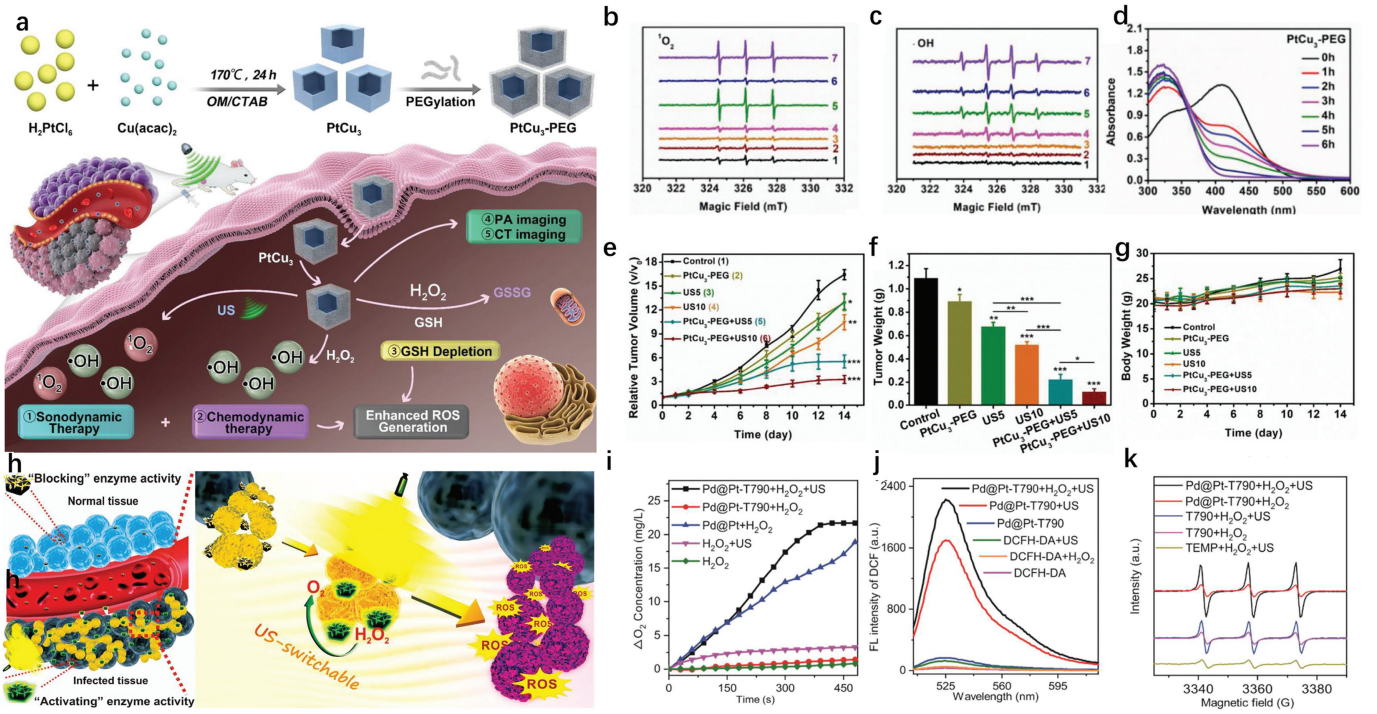

Fig. 7. (a) Schematic illustration of photoacoustic (PA)/computed tomography (CT) dual-modal imaging guided cancer chemodynamic therapy (CDT) and GSH depletion enhanced sonodynamic therapy (SDT) by $PtCu_3$ nanocages. ESR spectra of (b) TEMP/$^1O_2$ and (c) DMPO/ $HO^{\bullet}$ adducts in different solutions. The seven groups were 1) $PtCu_3$-PEG, 2) H_2O_2, 3) US, 4) $PtCu_3$-PEG + H_2O_2, 5) $PtCu_3$-PEG + US, 6) H_2O_2 + US, and 7) $PtCu_3$-PEG + H_2O_2 + US, respectively. (d) GSH depletion of different solutions with DTNB as the trapping agent. (e) Tumor growth curves of mice. (f) Tumor weights at the endpoint of the treatment schedule. (g) Body weights changes during the treatment. Reprinted with permission [133]. Copyright 2019, John Wiley and Sons. (h) Schematic illustration of the mechanism of US-switchable Pd@Pt-T790 nanoplatform for oxygen-generation-enhanced SDT of bacterial infection. (i) O_2 generation by Pd@Pt-T790 with or without US irradiation. (j) Fluorescence changes of DCFH-DA in the presence of different materials upon US irradiation. (k) Electron spin resonance spectra of $^1O_2$ trapped by 2,2,6,6-tetramethylpiperidine after US irradiation. Reprinted with permission [134]. Copyright 2019, American Chemical Society.

framework-67 (ZIF-67) nanoparticles. For H_2O_2 generation, this system could mimic SOD activity to convert $O_2^{\bullet-}$ into H_2O_2 (Figs. 8b and c). For H_2O_2 accumulation, the CAT inhibitor 3-AT could be released to inhibit the activity of CAT and weaken the decomposition of H_2O_2. In addition, PZIF67-AT was able to deplete GSH to avoid the H_2O_2 consumption caused by GPx or GSH (Figs. 8d and e). The elevation of H_2O_2 could enhance the Fenton reaction for the generation of more $HO^{\bullet}$ to induce cellular oxidative damage and eradicate tumors (Figs. 8f–h).

Glucose oxidase activity is also a candidate to enhance CDT, as it can elevate the H_2O_2 concentration and slightly lower the local pH through the generation of gluconic acid. Based on this principal, many nanoplatforms have been designed to improve the CDT. Chen *et al.* integrated a biodegradable dendritic mesoporous silica nanoparticles (DMSNs) with natural glucose oxidase (GOD) and ultrasmall Fe_3O_4 NPs to form a composite GOD-Fe_3O_4@DMSNs nanocatalyst (GFD NCs) [141]. GOD catalyzed glucose into abundant H_2O_2, which was further catalyzed by Fe_3O_4 NPs to liberate toxic ROS and induce tumor cell apoptosis. Recently, based on the similar mechanism, Han's group also designed a Co-ferrocene metal-organic framework (Co-Fc NMOF) with the incorporation of glucose oxidase, named (Co-Fc@GOx) [142]. Co-Fc acted as the Fenton-like agent to generate $HO^{\bullet}$ with the assistance of GOD, enabling an amplified CDT efficiency. The glucose oxidase could also be replaced by oxidase-mimicking nanozymes, such as gold NPs for realizing a similar therapeutic outcome [143].

3.3.5. Other multimodal synergistic therapy

Because of the complicated TME, tumors are easy to proliferate and metastasize, which makes it hard to eradicate tumors *via* a monotherapy. Consequently, "all in one" therapeutic nanoplatforms with multiple synergistic therapies are coming out to achieve improved therapeutic effects. For example, Lin *et al.* designed a hollow mesoporous Cu_2MoS_4 (CMS) loaded with glucose oxidase (GOx) [144]. The CMS exhibited Fenton-like, catalase-like, and glutathione (GSH) depletion activities because of the multivalent elements ($Cu^{1+/2+}$, $Mo^{4+/6+}$). When been internalized into the tumor, CMS can generate $HO^{\bullet}$ through Fenton reaction for CDT, while the GOx can deplete glucose to realize a starvation therapy. Meanwhile, the high photothermal conversion efficiency (η = 63.3%) under 1064 nm laser irradiation allowed CMS to have an excellent $O_2^{\bullet-}$ generation capability. Besides, CMS was further combined with anti-cytotoxic T-lymphocyte antigen-4 (CTLA4) checkpoint blockade to elicit robust immune response for tumor therapy. This multifunctional cascade bioreactor combined cancer CDT, PTT, PDT, starvation therapy and immunotherapy all together, receiving a remarkably enhanced efficacy to remove tumor and inhibit cancer metastasis. Xing and coworkers also constructed a synergetic Au_2Pt-PEG-Ce6 nanoformulation [145]. The Au_2Pt nanozymes possessed CAT and POD activities, which not only alleviated tumor hypoxia for enhanced PDT, but also produced $HO^{\bullet}$ for CDT. With a high photothermal conversion efficiency (η = 31.5%), this nanoformulation was able to realize photoacoustic (PA) and photothermal (PT) imaging guided PTT. In a word, the Au_2Pt-PEG-Ce6 integrated multimodal imaging-guided synergistic PTT/PDT/CDT together for a reinforced tumor therapy.

4. Nanozymes downregulating ROS for disease therapy

Under the normal physiological conditions, appropriate ROS is an important kind of messenger in regulating multiple cellular signaling pathways [146]. However, excessive ROS especially highly toxic species may disrupt the cellular redox homeostasis and damage the antioxidant defense system [147], which would destroy the structure and function of organisms and then lead to a series of diseases, such as neurodegenerative diseases (Parkinson's and Alzheimer's diseases), inflammation and aging. Nanozymes with

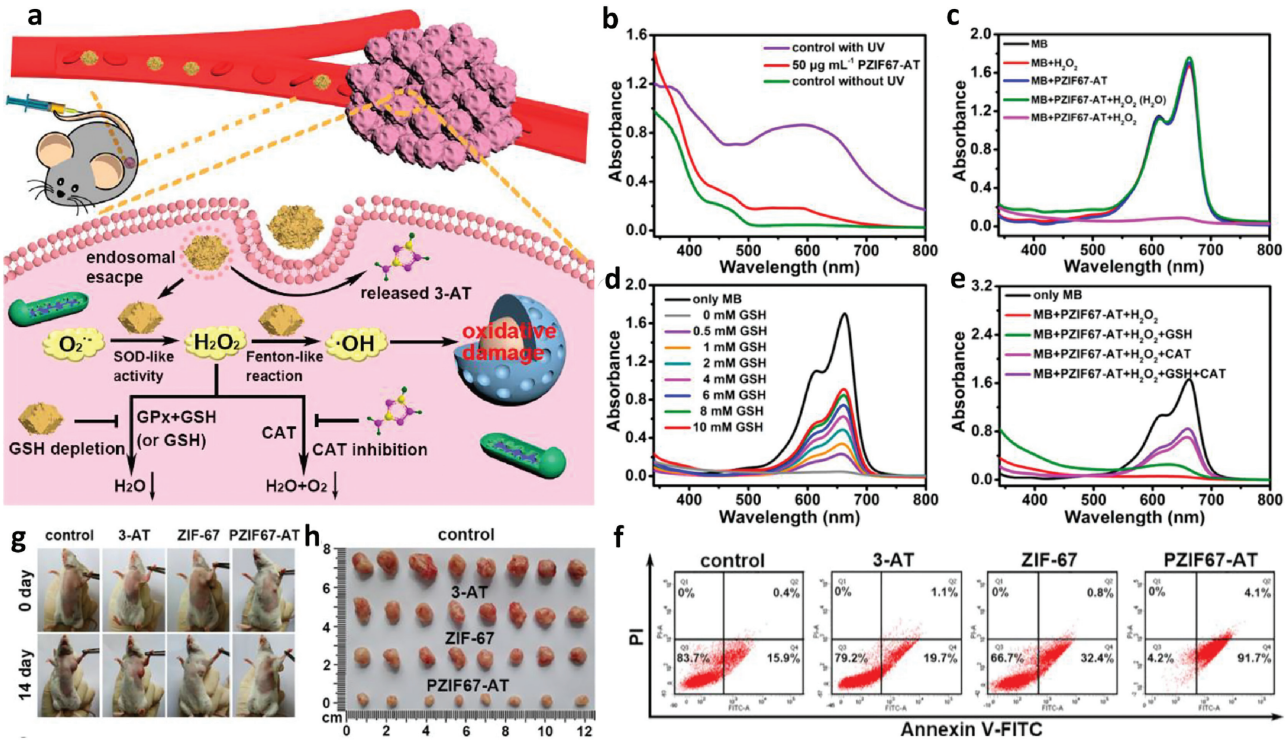

Fig. 8. (a) Schematic representation of PZIF67-AT nanoparticles to induce intensive CDT. (b) SOD-mimicking activity of PZIF67-AT. (c) Degradation of MB by the PZIF67-AT-mediated Fenton-like reaction. (d) Impact of different GSH concentrations on MB degradation (mM: mmol/L). (e) Influence of GSH and CAT on the MB degradation. (f) Fluorescein-annexin V and PI staining assays of HeLa cells. (g) Photos of the tumor-bearing mice before and after 14 days of treatments. (h) Photographs of the dissected tumors after treatments for 14 days. Reprinted with permission [140]. Copyright 2020, American Chemical Society.

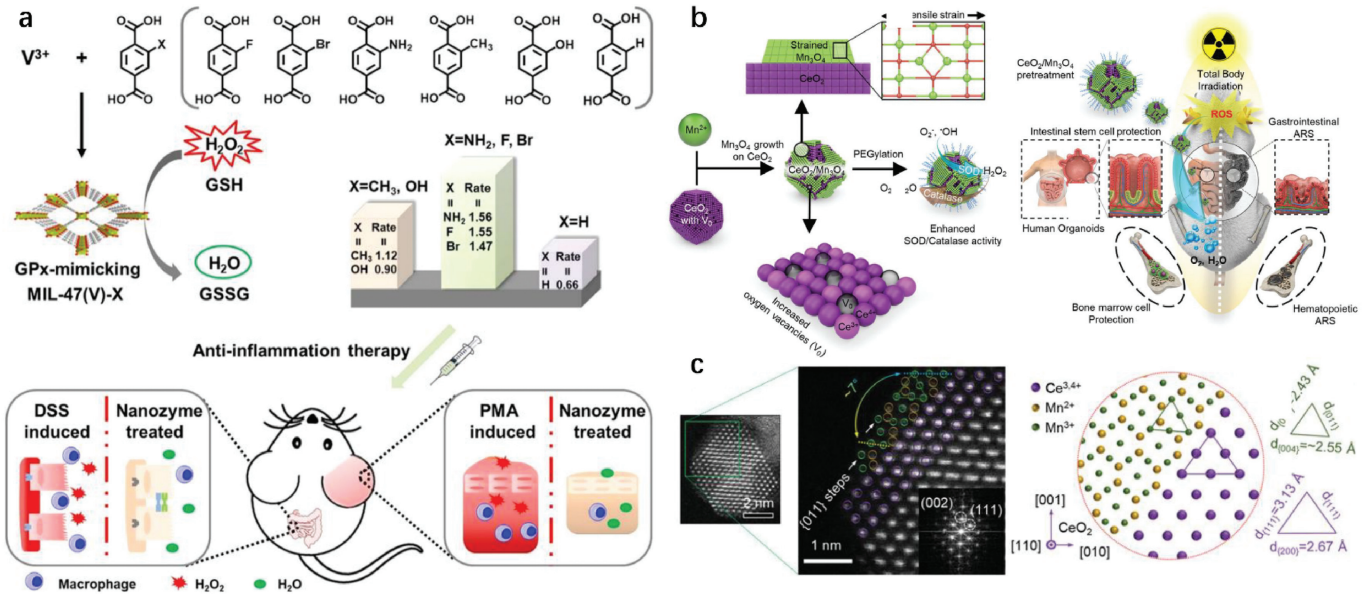

Fig. 9. (a) Illustration of the synthesis of GPx-mimicking MIL-47(V)-X MOF nanozymes for anti-inflammation therapy. Reprinted with permission [150]. Copyright 2020, John Wiley and Sons. (b) Schematic illustration of highly catalytic CeO_2/Mn_3O_4 nanocrystals preventing acute radiation syndrome. (c) Atomic resolution STEM images of CeO_2/Mn_3O_4 nanocrystals. Reprinted with permission [151]. Copyright 2020, John Wiley and Sons.

CAT or SOD activities are able to eliminate toxic H_2O_2 and $O_2^{\bullet-}$, respectively, and GPx can also consume H_2O_2. In another word, nanozymes could directly down-regulate excessive ROS and relieve local oxidative stress. Metallic oxide nanozymes, such as manganese oxide [148], cerium oxide [72] and vanadium oxide [149] have attracted great attention for their antioxidant properties.

4.1. Single-enzyme-like strategy

GPx is a critical antioxidant enzyme that could convert H_2O_2 to nontoxic H_2O. Wei's group developed a GPx nanozyme by using metal-organic frameworks (MOF) to rationally modulate the enzyme activity though a ligand engineering strategy [150]. They used 1,4-benzenedicarboxylicacid (BDC) with different substituents to construct MIL-47(V)-X (MIL stands for Materials of Institute Lavoisier; X = F, Br, NH_2, CH_3, OH, and H) MOFs (Fig. 9a). The GPx-mimicking activity was from the vanadium nodes of the MOFs, while the substitution of BDC could tune the electronic properties to modulate the final enzyme activity. Among the six MOFs, MIL-47(V)-NH_2 was found to exhibit the highest GPx activity because its V species were less oxidized, which made it react with H_2O_2 more easily to enhance the GPx activity. This MOF GPx nanozyme was efficiently applied to both ear inflammation and colitis.

Nanozymes with SOD activity can convert superoxide to less-oxidizing hydrogen peroxide and oxygen to relieve oxidative stress. In mammalian cells, there are three kinds of SOD, cytosolic SOD (SOD1 or Cu-Zn-SOD), mitochondrial SOD (SOD2 or Mn-SOD) and extracellular SOD (SOD3 or Cu-Zn-SOD), which regulate the organelle-specific activity and redox signaling. Recently, Mugesh's group reported a cerium vanadate ($CeVO_4$) nanorods to precisely function as SOD1 and SOD2 [151]. After being treated with $CeVO_4$, neuron cells with gene silencing of SOD1 and SOD2 can improve the level of pro-survival B cell lymphoma 2 (Bcl-2) family proteins, and restore the mitochondrial integrity to increase the ATP level under oxidative conditions, respectively. This nanozyme can fully substitute natural enzyme to treat mitochondrial dysfunction.

4.2. Multi-enzyme-like strategy

Nanozymes with both SOD and CAT activity could perform as a cascade reaction system to exhibit synergistic ROS-scavenging activity. Recently, Hyeon's group constructed CeO_2/Mn_3O_4 nanocrystals with enhanced SOD and CAT catalytic reactivity (Fig. 9b) [152]. A Mn_3O_4 nanolayer was formed on the surface of CeO_2 nanocrystals by a seed-mediated growth process. Because of the large lattice mismatch (13%) between CeO_2 {200} and Mn_3O_4 {004} (2.71 and 2.36 Å, respectively), Mn_3O_4 experienced a tensile strain to expand lattice (~2.55 Å) (Fig. 9c). The strained Mn_3O_4 layer increased oxygen vacancies in the CeO_2 phase, which significantly raised the oxygen adsorption efficiency of the nanocrystal surface. As a result, the SOD and CAT activity of the heterostructured CeO_2/Mn_3O_4 nanocrystals was greatly improved, allowing it to scavenge ROS with a lower dose and inducing slighter side effects. This powerful ROS scavenger was efficient enough to protect the regenerative capability of intestinal stem cells and increase the survival rate of mice after a lethal dose of irradiation.

Wei *et al.* designed an integrated SOD/CAT cascade nanozyme (Pt@PCN222-Mn) by introducing Mn(III) porphyrin and Pt within a Zr-based MOF(PCN22) [153]. Mn(III) porphyrin functioned as the SOD-like moiety while Pt served as the CAT-like moiety. Compared with PCN22 doped with only Mn(III) porphyrin or only Pt, the cascade nanozyme Pt@PCN222-Mn exhibited improved SOD and CAT activities due to the synergistic effect between Mn(III) porphyrin and Pt NPs. The synergistic effect was attributed to the pore confinement effect of PCN22 MOF. High dense Pt NPs were constrained in PCN22 without the aggregation to lose their activity, which greatly enhanced the CAT property. As for the SOD activity, the generated H_2O_2 would interact with Mn nuclei to occupy the active sites and block the combination with a new $O_2^{\bullet-}$. Thus, the Pt NPs confined near Mn sites could consume H_2O_2 to accelerate the reaction rate. The synergistic ROS-scavenging capacity of this cascade nanozyme endowed it with superior therapeutic efficacy toward two forms of inflammatory bowel disease (IBD), *i.e.*, ulcerative colitis and Crohn's disease.

Further researches combined SOD, CAT and GPx three kinds of enzyme activities all together to exhibit the maximal synergetic ROS-scavenging effects. Ren *et al.* reported a nitrogen-doped carbon supported single-atom catalysts (SACs) with atomically dispersed Co-porphyrin centers (Co/PMCS) (Fig. 10a) [100]. Due to the coordinatively unsaturated active metal centers similar with metalloenzymes, Co/PMCS could successfully mimicked CAT, SOD and GPx to eliminate H_2O_2, $O_2^{\bullet-}$ and $HO^{\bullet}$ (Figs. 10b–e). Additionally, they demonstrated that $NO^{\bullet}$ could react fast with SACs *via* the coordination with the Co-porphyrin centers. This Co/PMCS provided a powerful elimination ability of reactive oxygen and nitrogen species (RONS) for alleviating the systematic inflammatory response and reducing multiple organ dysfunction in the LPS-induced sepsis and bacteremia mice (Figs. 10f–i).

Lately, Chen *et al.* used Cu^{2+} and L-ascorbic acid (AA) to fabricate ultrasmall $Cu_{5.4}O$ nanoparticles ($Cu_{5.4}O$ USNPs) with the above three kinds of enzymes (SOD, CAT and GPx) activities to realize a broad-spectrum ROS scavenging [154]. The prepared $Cu_{5.4}O$ USNPs with an average diameter of 3.5−4 nm had an excellent biocompatibility and a high renal clearance ability. Importantly, the remarkable ROS scavenging efficiency allowed it be applicable to AKI (acute kidney injury), ALI (acute lung injury), and diabetic wound pathological conditions. Its ultrasmall size guaranteed an extremely low working concentration to reduce the side effects (about 25 ng/mL *in vitro* and 2 μg/kg for acute kidney injury *in vivo*), which was at least two orders magnitude lower than the other reported antioxidant nanozymes.

Other nanozymes could also remove reactive nitrogen species (RNS) (*e.g.*, $NO^{\bullet}$ and ONOO−). RNS is also a kind of free radicals with strong oxidative ability. Zhang *et al.* developed a trimetallic (triM) nanozyme using Pt, Pd and Mo [155]. Because of the lattice distortion and exposure of active sites, the triM nanozymes with POD and CAT activities possessed an enhanced antioxidant property for removing ROS and RNS. Besides metal and metal oxide, Tian *et al.* also produced a hollow Prussian blue nanozymes (HPBZs) with multi-enzyme-like activities (POD and SOD) though a Bi^{3+} assisted, template-free synthetic strategy. The hollow structure and large surface area of HPBZs endowed it with high adsorption of RONS, which notably improved its RONS scavenging ability for the ischemic injury treatment [156].

5. Challenges and future opportunities

As potential substitutes of natural enzymes, nanozymes from rationally engineered nanomaterials have gained increasing attentions over the past decade. Remarkable achievements have been made for the design and application of nanozymes in therapy of over ten kinds of disease. Based on the rapid developments and innovations, this review summarizes the typical catalytic mechanisms of engineered nanomaterials as nanozymes and highlights the representative strategies on how nanozymes can modulate ROS level for therapy of different kinds of diseases. The related diseases include these that could be destroyed from ROS generation such as cancer and pathogen infection, and those that could benefit from ROS scavenging such as inflammation and neurodegeneration. Although with bright prospects, this newly emerging field still has numerous challenges to be tackled.

First, the catalytic activity and substrate specificity of current nanozymes are still far from optimal. Compared with natural enzymes, the performances of these two nanozymes characters are relatively low. Only with an excellent catalytic ability, the dose of nanozymes could be reduce and relieve the possible side effects. Due to their lack of surface binding pockets, nanozymes usually have a class instead of only one specific substrate, which greatly hinders their molecular recognition function. Rational design and functionalization of the nanomaterials should be further explored

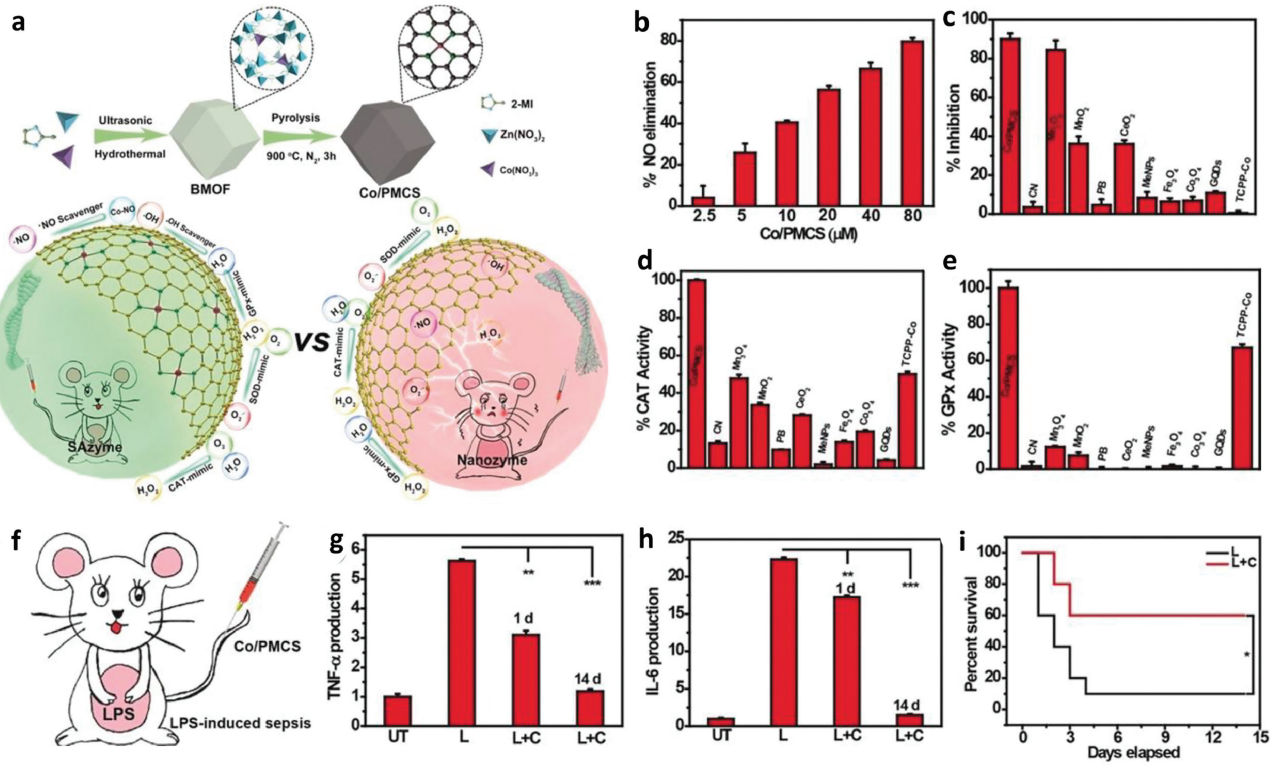

Fig. 10. (a) Schematic illustration of the formation of Co/PMCS and their application as multi-antioxidant SAzymes for sepsis management. (b) $NO^{\bullet}$-scavenging activity. (d-f) A comparison of the SOD-like, CAT-like, GPx-like activities of Co/PMCS with other antioxidative materials. (f) Illustration of the *in vivo* LPS-induced sepsis model. (g) TNF-α and (h) IL-6 *in vivo* in different groups. (i) Survival curves of the two groups observed for 14 days. Reprinted with permission [100]. Copyright 2020, John Wiley and Sons.

to improve the catalytic performance. To solve these problems, surface modification is a pathway to enhance the catalytic performance. By coating functional elements, the binding affinity with substrate and the contact between nanozymes and substrates could be improved. Moreover, it is also feasible to build specific binding pockets to increase the catalytic specificity through surface modification.

Second, the catalytic mechanisms need to be fully recognized. Although the functions of nanozymes are widely investigated, their specific catalytic mechanisms have not been clearly understood yet. The catalytic mechanisms of different nanomaterials are also different. To date, only a few catalytic processes of nanozymes have been detailedly reported and the synergistic mechanisms between multi-enzyme-like activities are rarely studied. Thus, it is imperative to systematically establish a complete theoretical system of nanozymes. Currently, the combination of theoretical calculation and experimental verification is a compromised but effective pathway to understand the kinetics and mechanisms. For example, DFT investigation is a popular method to predict the electronic structure and energy transition.

Third, nanozymes with more types of catalytic activities should be designed and fabricated for broader biological and biomedical applications. Up to now, most nanozymes are oxidoreductases and hydrolases, while other kinds of enzymes, such as transferases and lyasesare still lack. As a result, it is essential to develop nanomaterials that could mimic more kinds of natural enzyme activities. Thus, broader applications of these nanomaterials could be realized. The unique properties make nanozymes for both *in vitro* and *in vivo* applications. A few years ago, the applications of nanozymes mainly focused on detection and environmental remediation. Recently, *in vivo* diagnosis and treatment become the new hot topic. However, there are still a lot to be done, not only in biomedicine and environment, but also in food health and agriculture. Besides, the development in existing fields should also be further expanded, such as applications in tissue engineering [72], drug screening [157] and regenerative medicine [158].

Last but not the least, the biological effect and biosafety of the nanozymes should be thoroughly evaluated. Unlike natural enzymes, nanozymes might have potential toxicity due to the nanosized effect and the included toxic components. As a result, the biological fates of the nanozymes should be monitored before possible clinical transformation, including cytotoxicity, immunogenicity, pharmacokinetics, metabolism and *in vivo* biodistribution.

Declaration of competing interest

The authors declare that they have no known competing financial interests or personal relationships which have or could be perceived to have influenced the work reported in this article.

Acknowledgments

The work was supported by the National Key R&D project from Minister of Science and Technology, China (No. 2016YFA0202703), the National Nature Science Foundation (Nos. 82072065, 81471784), the Nature Science Foundation of Beijing (No. 2172058), and the National Youth Talent Support Program.

References

[1] A.W. Dobson, Y. Xu, M.R. Kelley, et al., J. Biol. Chem. 275 (2000) 37518–37523.
[2] H. Beinert, D.E. Green, P. Hele, et al., Science 124 (1956) 614–615.
[3] C.N. Serhan, A. Jain, S. Marleau, et al., J. Immunol. 171 (2003) 6856–6865.
[4] S.C. Lu, Mol. Aspects Med. 30 (2009) 42–59.
[5] D.M. Shih, L.J. Gu, Y.R. Xia, et al., Nature 394 (1998) 284–287.
[6] C. Mateo, J.M. Palomo, G.F. Lorente, et al., Enzyme Microb. Technol. 40 (2007) 1451–1463.
[7] M. Liang, X. Yan, Acc. Chem. Res. 52 (2019) 2190–2200.
[8] F. Manea, F.B. Houillon, L. Pasquato, P. Scrimin, Angew. Chem. Int. Ed. 43 (2004) 6165–6169.
[9] L. Gao, J. Zhuang, L. Nie, et al., Nat. Nanotechnol. 2 (2007) 577–583.
[10] B. Liu, Z. Sun, P.J. Huang, J. Liu, J. Am. Chem. Soc. 137 (2015) 1290–1295.
[11] F. Wang, Y. Zhang, Z. Liu, et al., Nanoscale 12 (2020) 14465–14471.
[12] W. Yin, J. Yu, F. Lv, et al., ACS Nano 10 (2016) 11000–11011.
[13] K. Zhang, M. Tu, W. Gao, et al., Nano Lett. 19 (2019) 2812–2823.
[14] C. Liu, J. Xing, O.U. Akakuru, et al., Nano Lett. 19 (2019) 5674–5682.
[15] R. Yan, S. Sun, J. Yang, et al., ACS Nano 13 (2019) 11552–11560.
[16] M.P. Murphy, Biochem. J. 417 (2009) 1–13.
[17] C.C. Winterbourn, Nat. Chem. Biol. 4 (2008) 278–286.
[18] V.J. Thannickal, B.L. Fanburg, Am. J. Physiol. Lung Cell Mol. Physiol. 279 (2000) L1005–L1028.
[19] S.S. Gill, N. Tuteja, Plant Physiol. Biochem. 48 (2010) 909–930.
[20] H. Pelicano, D. Carney, P. Huang, Drug Resist. Updat. 7 (2004) 97–110.
[21] E.R. Stadtman, Free Radical Res. 40 (2006) 1250–1258.
[22] K. Ito, A. Hirao, F. Arai, et al., Nat. Med. 12 (2006) 446–451.
[23] M. Mittal, M.R. Siddiqui, K. Tran, et al., Antioxid. Redox Signal. 20 (2014) 1126–1167.
[24] F. Giacco, M. Brownlee, Circul. Res. 107 (2010) 1058–1070.
[25] M. Brownlee, Diabetes 54 (2005) 1615–1625.
[26] W.R. Markesbery, Free Radical Biol. Med. 23 (1997) 134–147.
[27] K. Apel, H. Hirt, Annu. Rev. Plant Biol. 55 (2004) 373–399.
[28] Z. Zhou, J. Song, L. Nie, X. Chen, Chem. Soc. Rev. 45 (2016) 6597–6626.
[29] X. Qian, Y. Zheng, Y. Chen, Adv. Mater. 28 (2016) 8097–8129.
[30] S. Wang, G. Yu, Z. Wang, et al., Angew. Chem. Int. Ed. 58 (2019) 14758–14763.
[31] P. Sonveaux, Oncotarget 8 (2017) 35482–35483.
[32] M. Hu, K. Korschelt, P. Daniel, et al., ACS Appl. Mater. Interfaces 9 (2017) 38024–38031.
[33] X. Mu, J. Wang, Y. Li, et al., ACS Nano 13 (2019) 1870–1884.
[34] Y. Huang, C. Liu, F. Pu, et al., Chem. Commun. 53 (2017) 3082–3085.
[35] D. Li, B. Liu, P.J.J. Huang, et al., Chem. Commun. 54 (2018) 12519–12522.
[36] K. Fan, H. Wang, J. Xi, et al., Chem. Commun. 53 (2017) 424–427.
[37] D. Jiang, D. Ni, Z.T. Rosenkrans, et al., Chem. Soc. Rev. 48 (2019) 3683–3704.
[38] M. Liang, X. Yan, Acc. Chem. Res. 52 (2019) 2190–2200.
[39] X. Shen, Z. Wang, X. Gao, Y. Zhao, ACS Catal. 10 (2020) 12657–12665.
[40] Y. Ding, G. Wang, F. Sun, Y. Lin, ACS Appl. Mater. Interfaces 10 (2018) 32567–32578.
[41] Z. Wang, X. Shen, X. Gao, Y. Zhao, Nanoscale 11 (2019) 13289–13299.
[42] S. Guo, L. Guo, J. Phys. Chem. C 123 (2019) 30318–30334.
[43] D. Wang, X. Song, P. Li, et al., J. Mater. Chem. B 39 (2020) 9028–9034.
[44] X. Gonze, B. Amadon, P.M. Anglade, et al., Comput. Phys. Commun. 180 (2009) 2582–2615.
[45] X. Wang, X.J. Gao, L. Qin, et al., Nat. Commun. 10 (2019) 704.
[46] S. Guo, L. Guo, J. Phys. Chem. C 123 (2019) 30318–30334.
[47] A.C. Moreno Maldonado, E.L. Winkler, M. Raineri, et al., J. Phys. Chem. C 123 (2019) 20617–20627.
[48] B. Jiang, D. Duan, L. Gao, et al., Nat. Protoc. 13 (2018) 1506–1520.
[49] Z. Zhang, X. Zhang, B. Liu, J. Liu, J. Am. Chem. Soc. 139 (2017) 5412–5419.
[50] S.B. Bankar, M.V. Bule, R.S. Singhal, L. Ananthanarayan, Biotechnol. Adv. 27 (2009) 489–501.
[51] R. Ragg, F. Natalio, M.N. Tahir, et al., ACS Nano 8 (2014) 5182–5189.
[52] S.G. Rhee, Science 312 (2006) 1882–1883.
[53] X. Mei, T. Hu, H. Wang, et al., Biomaterials 258 (2020) 120257.
[54] M. Comotti, C. Della Pina, R. Matarrese, M. Rossi, Angew. Chem. Int. Ed. 43 (2004) 5812–5815.
[55] M. Comotti, C. Della Pina, E. Falletta, M. Rossi, Adv. Synth. Catal. 348 (2006) 313–316.
[56] X. Shen, W. Liu, X. Gao, et al., J. Am. Chem. Soc. 137 (2015) 15882–15891.
[57] Q. Wang, G. Hong, Y. Liu, et al., RSC Adv. 10 (2020) 25209–25213.
[58] Y. Yang, D. Zhu, Y. Liu, et al., Nanoscale 12 (2020) 13548–13557.
[59] F. Charbgoo, M. Bin Ahmad, M. Darroudi, Int. J. Nanomedicine 12 (2017) 1401–1413.
[60] J. Yao, Y. Cheng, M. Zhou, et al., Chem. Sci. 9 (2018) 2927–2933.
[61] S.M. Hirst, A.S. Karakoti, R.D. Tyler, et al., Small 5 (2009) 2848–2856.
[62] T. Pirmohamed, J.M. Dowding, S. Singh, et al., Chem. Commun. (Camb.) 46 (2010) 2736–2738.
[63] S. Singh, Biointerphases 11 (2016) 04B202.
[64] I. Celardo, J.Z. Pedersen, E. Traversa, L. Ghibelli, Nanoscale 3 (2011) 1411–1420.
[65] P. Ji, L. Wang, F. Chen, J. Zhang, ChemCatChem 2 (2010) 1552–1554.
[66] D. Damatov, J.M. Mayer, Chem. Commun. (Camb.) 52 (2016) 10281–10284.
[67] V. Nicolini, E. Gambuzzi, G. Malavasi, et al., J. Phys. Chem. B 119 (2015) 4009–4019.
[68] I.N. Zelko, T.J. Mariani, R.J. Folz, Free Radical Biol. Med. 33 (2002) 337–349.
[69] A. Okado-Matsumoto, I. Fridovich, J. Biol. Chem. 276 (2001) 38388–38393.
[70] J.M. McCord, M.A. Edeas, Biomed. Pharmacother. 59 (2005) 139–142.
[71] S. Liu, R. Tian, J. Xu, et al., Chem. Commun. 55 (2019) 13820–13823.
[72] Y. Guan, M. Li, K. Dong, et al., Biomaterials 98 (2016) 92–102.
[73] Y. Sheng, I.A. Abreu, D.E. Cabelli, et al., Chem. Rev. 114 (2014) 3854–3918.
[74] E.G. Heckert, A.S. Karakoti, S. Seal, W.T. Self, Biomaterials 29 (2008) 2705–2709.

[75] G. Calabrese, B. Morgan, J. Riemer, Antioxid. Redox Signal. 27 (2017) 1162–1177.
[76] E.V. Kalinina, N.N. Chernov, M.D. Novichkova, Biochemistry (Mosc.) 79 (2014) 1562–1583.
[77] N. Couto, J. Wood, J. Barber, Free Radical Biol. Med. 95 (2016) 27–42.
[78] O.M. Ighodaro, O.A. Akinloye, Alex. J. Med. 54 (2018) 287–293.
[79] R. Brigelius-Flohe, M. Maiorino, Biochim. Biophys. Acta 1830 (2013) 3289–3303.
[80] M.M. Gaschler, A.A. Andia, H. Liu, et al., Nat. Chem. Biol. 14 (2018) 507–515.
[81] M. Jia, D. Qin, C. Zhao, et al., Nat. Immunol. 21 (2020) 727.
[82] L.J. Yant, Q.T. Ran, L. Rao, et al., Free Radical Biol. Med. 34 (2003) 496–502.
[83] Y. Huang, Z. Liu, C. Liu, et al., Chem. Eur. J. 24 (2018) 10224–10230.
[84] T. Wirth, Angew. Chem. Int. Ed. 54 (2015) 10074–10076.
[85] Y. Huang, C. Liu, F. Pu, et al., Chem. Commun. (Camb.) 53 (2017) 3082–3085.
[86] N. Singh, M.A. Savanur, S. Srivastava, et al., Angew. Chem. Int. Ed. 56 (2017) 14267–14271.
[87] A.A. Vernekar, D. Sinha, S. Srivastava, et al., Nat. Commun. 5 (2014) 5301.
[88] S. Ghosh, P. Roy, N. Karmodak, et al., Angew. Chem. Int. Ed. 57 (2018) 4510–4515.
[89] B. Yang, Y. Chen, J. Shi, Chem. Rev. 119 (2019) 4881–4985.
[90] V.D. Petrov, F. van Breusegem, AoB Plants (2012) pls014.
[91] H. Sies, Redox Biol. 11 (2017) 613–619.
[92] G.P. Bienert, A.L.B. Moller, K.A. Kristiansen, et al., J. Biol. Chem. 282 (2007) 1183–1192.
[93] L. Huang, J.X. Chen, L.F. Gan, et al., Sci. Adv. 5 (2019) 9.
[94] J. Chen, H. Gao, Z. Li, et al., Chin. Chem. Lett. 31 (2020) 1398–1401.
[95] B. Xu, H. Wang, W. Wang, et al., Angew. Chem. Int. Ed. 58 (2019) 4911–4916.
[96] P. Wang, S. Liu, M. Hu, et al., Adv. Funct. Mater. 30 (2020) 2000647.
[97] F. Cao, L. Zhang, H. Wang, et al., Angew. Chem. Int. Ed. 58 (2019) 16236–16242.
[98] Y. Tao, E. Ju, J. Ren, X. Qu, Adv. Mater. 27 (2015) 1097–1104.
[99] A. Liu, M. Li, J. Wang, et al., Chin. Chem. Lett. 31 (2020) 1133–1136.
[100] F. Cao, L. Zhang, Y. You, et al., Angew. Chem. Int. Ed. 59 (2020) 5108–5115.
[101] K. Fan, J. Xi, L. Fan, et al., Nat. Commun. 9 (2018) 1440.
[102] Y. Huang, Z. Liu, C. Liu, et al., Angew. Chem. Int. Ed. 55 (2016) 6646–6650.
[103] J. Shan, X. Li, K. Yang, et al., ACS Nano 13 (2019) 13797–13808.
[104] X. Liu, Z. Yan, Y. Zhang, et al., ACS Nano 13 (2019) 5222–5230.
[105] Z. Wang, Y. Zhang, E. Ju, et al., Nat. Commun. 9 (2018) 3334.
[106] Q. Wu, Z. He, X. Wang, et al., Nat. Commun. 10 (2019) 240.
[107] M. Qi, H. Pan, H. Shen, et al., Angew. Chem. Int. Ed. 59 (2020) 11748–11753.
[108] C. Wei, Y. Liu, X. Zhu, et al., Biomaterials 238 (2020) 119848.
[109] W. Zhen, Y. Liu, W. Wang, et al., Angew. Chem. Int. Ed. 59 (2020) 9491–9497.
[110] Y. Liu, P. Bhattarai, Z. Dai, X. Chen, Chem. Soc. Rev. 48 (2019) 2053–2108.
[111] L. Minai, D.Y. Hayon, D. Yelin, Sci. Rep. 3 (2013) 2146.
[112] I.B. Slimen, T. Najar, A. Ghram, et al., Int. J. Hyperthermia 30 (2014) 513–523.
[113] L. Fan, X. Xu, C. Zhu, et al., ACS Appl. Mater. Interfaces 10 (2018) 4502–4511.
[114] M. Aioub, S.R. Panikkanvalappil, M.A. El-Sayed, ACS Nano 11 (2017) 579–586.
[115] S.P. Sun, C.J. Li, J.H. Sun, et al., J. Hazard. Mater. 161 (2009) 1052–1057.
[116] M. Wang, M. Chang, Q. Chen, et al., Biomaterials 252 (2020) 120093.
[117] M. Zhou, S. Song, J. Zhao, et al., J. Mater. Chem. B 3 (2015) 8939–8948.
[118] S. Shen, S. Wang, R. Zheng, et al., Biomaterials 39 (2015) 67–74.
[119] S. Li, L. Shang, B. Xu, et al., Angew. Chem. Int. Ed. 58 (2019) 12624–12631.
[120] Y. Jiang, X. Zhao, J. Huang, et al., Nat. Commun. 11 (2020) 1857.
[121] S. Dong, Y. Dong, T. Jia, et al., Adv. Mater. 32 (2020) 2002439.
[122] A.P. Castano, P. Mroz, M.R. Hamblin, Nat. Rev. Cancer 6 (2006) 535–545.
[123] J.P. Celli, B.Q. Spring, I. Rizvi, et al., Chem. Rev. 110 (2010) 2795–2838.
[124] M. Wu, Y. Ding, L. Li, Nanoscale 11 (2019) 19658–19683.
[125] Y. Zhang, F. Wang, C. Liu, et al., ACS Nano 12 (2018) 651–661.
[126] D. Wang, H. Wu, S.Z.F. Phua, et al., Nat. Commun. 11 (2020) 357.
[127] W. Hiraoka, H. Honda, L.B. Feril Jr., et al., Ultrason. Sonochem. 13 (2006) 535–542.
[128] H. Chen, X. Zhou, Y. Gao, et al., Drug Discov. Today 19 (2014) 502–509.
[129] J. Chen, H. Luo, Y. Liu, et al., ACS Nano 11 (2017) 12849–12862.
[130] X. Wang, X. Zhong, F. Gong, et al., Mater. Horizons 7 (2020) 2028–2046.
[131] F. Gong, L. Cheng, N. Yang, et al., Adv. Mater. 31 (2019) 1900730.
[132] P. Zhu, Y. Chen, J. Shi, ACS Nano 12 (2018) 3780–3795.
[133] X. Zhong, X. Wang, L. Cheng, et al., Adv. Funct. Mater. 30 (2019) 1907954.
[134] D. Sun, X. Pang, Y. Cheng, et al., ACS Nano 14 (2020) 2063–2076.
[135] M. Feng, Y. Pan, R. Kong, S. Shu, Innovation (New York, N.Y.) 1 (2020) 100032-100032.
[136] Z. Tang, Y. Liu, M. He, W. Bu, Angew. Chem. Int. Ed. 58 (2019) 946–956.
[137] Z. Tang, P. Zhao, H. Wang, et al., Chem. Rev. 121 (2021) 1981–2019.
[138] Y. Zhu, R. Zhu, Y. Xi, et al., Appl. Catal. B: Environ. 255 (2019) 117739.
[139] Y.S. Jung, W.T. Lim, J.Y. Park, Y.H. Kim, Environ. Technol. 30 (2009) 183–190.
[140] Y. Sang, F. Cao, W. Li, et al., J. Am. Chem. Soc. 142 (2020) 5177–5183.
[141] M. Huo, L. Wang, Y. Chen, J. Shi, Nat. Commun. 8 (2017) 357.
[142] C. Fang, Z. Deng, G. Cao, et al., Adv. Funct. Mater. 30 (2020) 1910085.
[143] H. Zhang, X. Liang, L. Han, F. Li, Small 14 (2018) 1803256.
[144] M. Chang, M. Wang, M. Wang, et al., Adv. Mater. 31 (2019) e1905271.
[145] M. Wang, M. Chang, Q. Chen, et al., Biomaterials 252 (2020) 120093.
[146] B. D'Autreaux, M.B. Toledano, Nat. Rev. Mol. Cell Biol. 8 (2007) 813–824.
[147] M.L. Circu, T.Y. Aw, Free Radical Biol. Med. 48 (2010) 749–762.
[148] N. Singh, M.A. Savanur, S. Srivastava, et al., Nanoscale 11 (2019) 3855–3863.
[149] Y. Huang, Z. Liu, C. Liu, et al., Angew. Chem. Int. Ed. 55 (2016) 6646–6650.
[150] J. Wu, Y. Yu, Y. Cheng, et al., Angew. Chem. Int. Ed. 60 (2020) 1227–1234.
[151] N. Singh, S.K. NaveenKumar, M. Geethika, G. Mugesh, Angew. Chem. Int. Ed. 60 (2020) 3121–3130.
[152] S.I. Han, S.W. Lee, M.G. Cho, et al., Adv. Mater. 32 (2020) 2001566.
[153] Y. Liu, Y. Cheng, H. Zhang, et al., Sci. Adv. 6 (2020) eabb2695.
[154] T. Liu, B. Xiao, F. Xiang, et al., Nat. Commun. 11 (2020) 2788.
[155] X. Mu, J. Wang, Y. Li, et al., ACS Nano 13 (2019) 1870–1884.
[156] K. Zhang, M. Tu, W. Gao, et al., Nano Lett. 19 (2019) 2812–2823.
[157] D. Duan, K. Fan, D. Zhang, et al., Biosens. Bioelectron. 74 (2015) 134–141.
[158] J. Park, J. Chu, A. Tsou, et al., Biomaterials 32 (2011) 3921–3930.